Eddy currents in the Alcator Tokamak

ASSOCIATIE EURATOM–FOM

FOM–INSTITUUT VOOR PLASMAFYSICA

RIJNHUIZEN – JUTPHAAS – NEDERLAND

March 1975

EDDY CURRENTS IN THE ALCATOR TOKAMAK

by

D.C. Schram* and J. Rem

Rijnhuizen Report 75 - 88

This work was performed as part of the research programme of the association agreement of Euratom and the "Stichting voor Fundamenteel Onderzoek der Materie" (FOM) with financial support from the "Nederlandse Organisatie voor Zuiver-Wetenschappelijk Onderzoek" (ZWO) and Euratom.

* Since 15 December 1972 at the Technical University of Eindhoven, The Netherlands.

C O N T E N T S

EDDY CURRENTS IN THE ALCATOR TOKAMAK

by

D.C. Schram* and J. Rem
Association Euratom-FOM
FOM-Instituut voor Plasmafysica
Rijnhuizen, Jutphaas, The Netherlands

ABSTRACT

A one-dimensional model of an aircore transformer is developed through which it is possible to analyse the effect of eddy currents in the primary windings - and of similar currents in the field coils for the toroidal magnetic field - on the time dependence of the current in a Tokamak experiment. The model is applied to the "Alcator" Tokamak at MIT and its accuracy is tested by comparing analytical results for the harmonic behaviour of the transformer, with experimental data. The time-dependent behaviour of the plasma current - for a constant plasma resistance - shows that eddy currents in the primary windings will lead to a reduction of 8% of the current maximum. The eddy currents in the "Bitter" coils are found to affect predominantly the initial current rise, they lead to a steepening of the current rise. Finally, the influence of the time dependence of the plasma resistance is investigated.

* Since 15 December 1972 at the Technical University of Eindhoven, The Netherlands.

1. INTRODUCTION

In toroidal plasma experiments of the Tokamak type the induction of a toroidal current in the plasma is an essential feature. This current heats the plasma and provides the poloidal magnetic field necessary for equilibrium and confinement. The magnetic flux requirements (in Vsec) for bringing the current up to a desired level and maintaining it for some time were until recently such that an iron core could be employed (cf. Fig. 1a). By this means an appreciable flux can be produced with a relatively small energizing primary current. This system has the advantage of a good coupling between the primary and the plasma, i.e., the control over the plasma current during the experiment is good.

Progress in the Tokamak research reflects itself in larger plasma currents for longer periods of time, this is especially true in high current density devices as Alcator. Consequently, the flux requirements increase to the point where an iron core would have to be driven beyond its saturation value. In that case an aircore transformer must be resorted too. Here, the primary current has to be appreciably higher to obtain the desired flux levels, and high stray fields do arise. Since stray fields at the plasma location are undesirable, a compensation system is required. Another disadvantage is the weak coupling between primary and secondary. Even when the primary is located near or on the plasma chamber (Fig. 1b) the coupling factor is of the order of $k^2 \simeq 0.7$, while with an iron core it is close to unity. Unfortunately, it is often impossible to locate the primary windings so close to the plasma. In that case they can only be placed in the centre bore around the axis of symmetry (Fig. 1c), which leads to an even weaker coupling between primary and secondary. The Alcator Tokamak at MIT's Francis Bitter National Magnet Laboratory has such an aircore transformer[1].

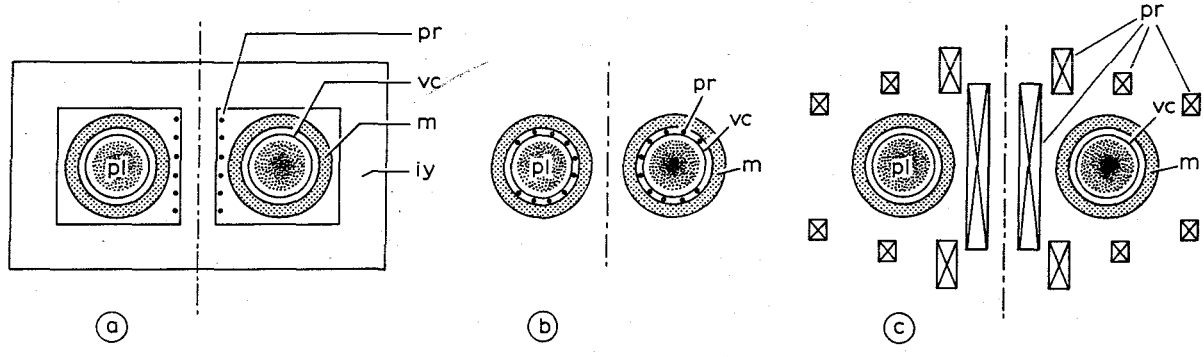

Fig. 1 Three Tokamak arrangements; iy = iron yoke, pr = primary windings, m = main magnetic field coils, vc = vacuum chamber, pl = plasma.

The high primary currents in an aircore transformer necessitate the use of primary windings with a large cross section. Therefore, changes of the primary and secondary currents will cause eddy currents to flow in the copper windings. In Alcator the thickness of the copper windings is such that the skin time is close to the desired primary time constant and to the rise time of the plasma current. As the copper volume is almost twice the air volume, these eddy currents will appreciably affect the rate of change of the primary flux and will lead to a decrease of the induced plasma current. Similarly, eddy currents in the copper of the coil for the toroidal magnetic field, which are of the Bitter type, will counteract a flux change induced by the plasma current. They cause an increase in the rate of change of the plasma current during the early phase of the discharge; the current maximum is only slightly reduced.

The effects of the eddy currents on the performance of the Alcator aircore transformer will be investigated on the basis of a model which we introduce in Sections 2 and 3. In Sections 4 and 5 we compare the harmonic behaviour of the transformer with measured data, while in Section 6 we analyse the time behaviour of the secondary current. In this presentation we focus our attention on the Alcator aircore transformer. The arguments, however, are general and can be applied to other geometries.

2. THE ALCATOR AIRCORE TRANSFORMER AND A MODEL

The Alcator device is designed to produce a plasma with electron densities up to 10^{14}/cc and temperatures of several keV for a time period of 100 - 200 msec. The estimated required flux is approximately 1 Vsec. The relevant components of the experiment are (Fig. 2) a toroidal vacuum vessel in which the plasma will be contained, a copper shell around the vacuum chamber, a toroidal Bitter coil for the main magnetic field, and the aircore transformer with compensation coils. All these components will be cooled to liquid nitrogen temperatures.

The main coil of the primary is built up out of 36 pancakes, each being a spiral of $6\frac{1}{3}$ turns of copper bar with a square cross section. The stray fields from the coil are compensated by the coils (C_1) each having 24 turns and two pairs of other coils (C_2) at a larger radius (Fig. 3).

The plasma forms the secondary winding of the aircore transformer. If the plasma current is assumed to be homogeneously distributed over the plasma cross section (radius r_p) the inductance of the plasma is:

$$L_2 \simeq \mu_o R_o \ln \left(1.38 \frac{R_o}{r_p}\right) H \quad , \tag{1}$$

where R_o is the major radius of the plasma toroid. With $R_o \sim 0.54$ m and $r_p \sim 0.10$ m we find $L_2 \simeq 1.37$ μH.

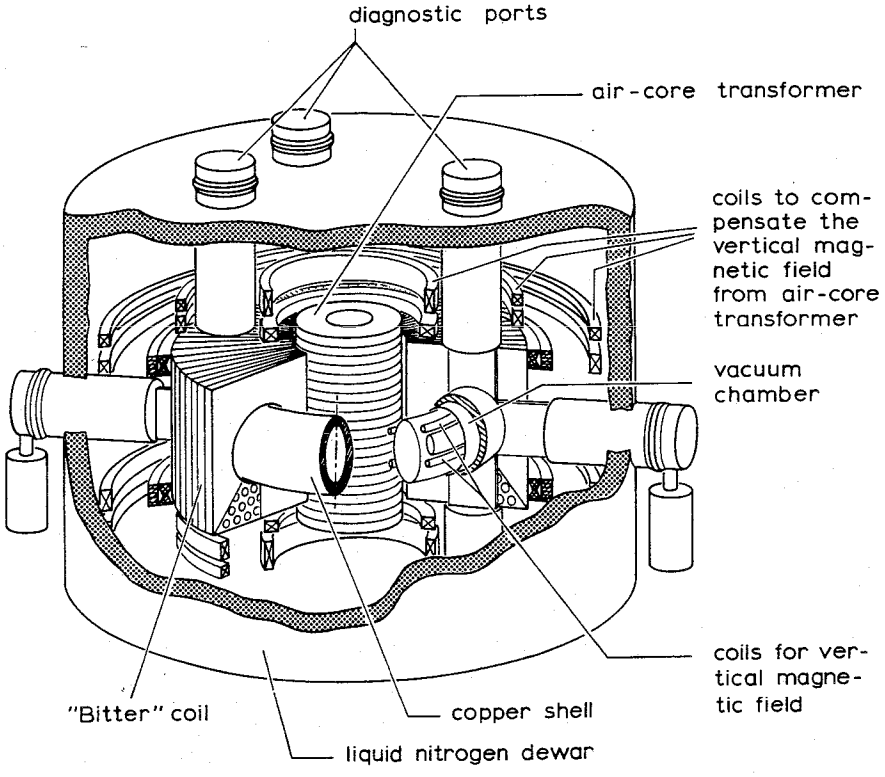

Fig. 2 The Alcator experiment.

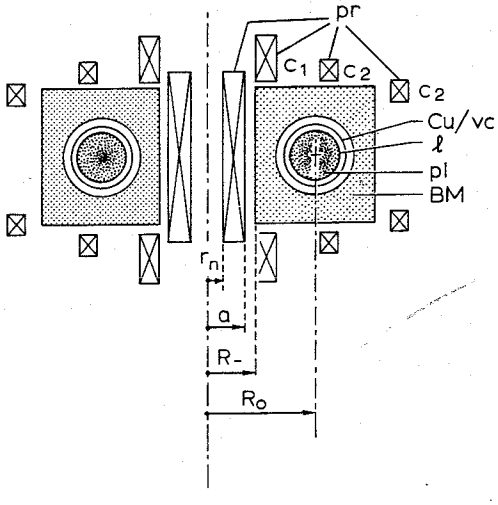

Fig. 3a

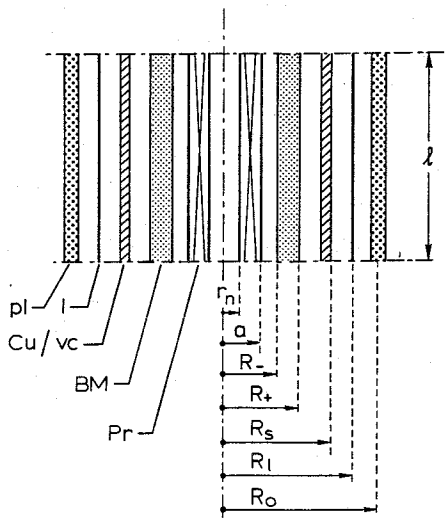

Fig. 3b

Sketches of the Alcator experiment and model.

pr = primary windings Cu = copper shell l = liner
BM = Bitter magnet vc = vacuum chamber pl = plasma

Dimensions are presented in Table I.

The compensation of the stray fields from the primary results in an apparent lengthening of the primary which permits us to introduce a model in which the primary can be considered as a section of an infinitely long coil. To account for the extra inductance introduced by the compensation coils, the effective length of the primary coil is taken 0.94 m instead of the actual length of 0.75, while the number of pancakes is taken as 45, i.e. 285 turns instead of 36, i.e. 228 turns. Furthermore, we shall approximate the helical windings of a pancake by circular windings connected in series (Fig. 4).

With the approximations made so far, the magnetic field of the transformer has become dependent on one dimension, the radius. Similarly, we shall approximate the secondary of the transformer so that also there the associated magnetic field depends only on the radius. This approximation is found by stretching the entire structure of vacuum shell, liner and plasma winding in the z-direction, i.e. by approximating it by a belt-pinch configuration. In this approximation the plasma is replaced by a cylindrical current sheath with no net current or flux in the z-direction and the vacuum shell and liner are replaced by coaxial cylinders (Fig. 3b).

The model described above, that of an infinite belt pinch, could have been analyzed per unit length. Instead of doing this we have taken a specific length: the effective length of the primary. In this way we can readily compare results between the model and the real transformer.

The inductance of the secondary winding in the model is chosen equal to the actual one: $L_2 \simeq 1.37$ μH; similarly, we have taken the inductance of the liner L_ℓ and that of the copper shell L_s to be equal to the actual ones, i.e.

$$L_\ell = \mu_o R_o \left[\ln \frac{8R_o}{r_\ell} - 2 \right] = \mu_o \pi R^2_{\ell\,\mathrm{eff}} \simeq 1.02\ \mu\mathrm{H} \quad ,$$

$$L_s = \mu_o R_o \left[\ln \frac{8R_o}{r_s} - 2 \right] = \mu_o \pi R^2_{s\,\mathrm{eff}} \simeq 0.90\ \mu\mathrm{H} \quad . \qquad (2)$$

Table I lists the actual geometrical quantities of the transformer and the effective values used in the model.

TABLE I

		Actual	Model
N	= number of pancakes	36	45
n	= number of windings per pancake	$6\frac{1}{3}$	$6\frac{1}{3}$
Nn	= total number of windings	228	285
ℓ/N	= height of one pancake	0.021 m	0.021 m
ℓ	= length of coil	0.75 "	0.94 "
$2d$	= thickness of winding	0.02 "	0.02 "
$a \equiv r_1$	= average radius of outer winding	0.22 "	0.22 "
R_o	= main radius of plasma column	0.54 "	0.57 "
r_p	= plasma radius	0.10 "	-
ℓ	= length of plasma sheath	-	0.94 "
R_+	= outer radius of Bitter magnet	-	0.45 "
R_-	= inner radius of Bitter magnet	0.24 "	0.24 "
R_s	= effective radius of copper shell (and vacuum vessel)	-	0.46 "
R_ℓ	= effective radius of liner	-	0.49 "

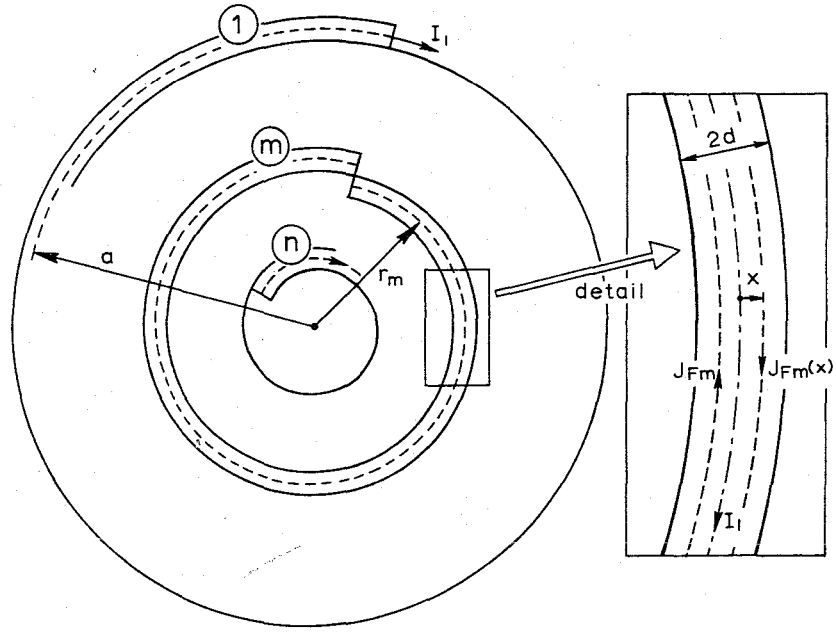

Fig. 4 Cross section of one pancake and detail.

3. THE EQUATIONS GOVERNING THE MODEL

The model introduced in the previous section is essentially one-dimensional, the magnetic field strength depends only on the radius.

Without eddy currents the transient response of the model is very simple: only the L/R times of the primary and of the secondary appear (cf. Section 6). The eddy currents, however, introduce two new time scales:
the skin time of the copper of the primary

$$\tau_s = \frac{\mu_o d^2}{2\eta} \quad , \tag{3a}$$

and the average skin time of the Bitter magnet

$$\tau_B = \frac{\mu_o d_B^2}{2\eta} \quad , \tag{3b}$$

where η is the resistivity of the copper and $2d_B$ is the average thickness of the Bitter plates. Eddy currents in the copper windings arise due to two effects: I_{F1} due to flux changes caused by the primary current I_1, and I_{F2} due to flux changes caused by the secondary current I_2. Since the response is linear, the total eddy current is the sum of these currents. The eddy current I_{FB} in the copper of the Bitter magnet can only be caused by changes in the secondary current, because the Bitter magnet is located outside the primary coil and no reverse flux is assumed to exist in our model. Using the definitions of Table II, we can write two equations in which we set the total applied and induced voltages equal to the resistive voltage drop, one equation for the pri-

TABLE II Definitions

flux change	caused by	as seen by
$\frac{d\phi_{11}}{dt}$, $\frac{d\phi_{11F}}{dt}$	$\frac{dI_1}{dt}$, $\frac{dI_{F1}}{dt}$	primary
$\frac{d\phi_{12}}{dt}$, $\frac{d\phi_{12F}}{dt}$	$\frac{dI_2}{dt}$, $\frac{dI_{F2}}{dt}$	"
$\frac{d\phi_{21}}{dt}$, $\frac{d\phi_{21F}}{dt}$	$\frac{dI_1}{dt}$, $\frac{dI_{F1}}{dt}$	secondary
$\frac{d\phi_{22}}{dt}$, $\frac{d\phi_{22F}}{dt}$	$\frac{dI_2}{dt}$, $\frac{dI_{F2}}{dt}$	"
$\frac{d\phi_B}{dt}$	$\frac{dI_{FB}}{dt}$	"

mary winding of the transformer and the other for the plasma:

$$\frac{d\phi_{11}}{dt} + \frac{d\phi_{11F}}{dt} + \frac{d\phi_{12}}{dt} + \frac{d\phi_{12F}}{dt} + R_1 I_1 = e_1 \quad , \tag{4a}$$

$$\frac{d\phi_{21}}{dt} + \frac{d\phi_{21F}}{dt} + \frac{d\phi_{22}}{dt} + \frac{d\phi_{22F}}{dt} + \frac{d\phi_B}{dt} + R_2 I_2 = 0 \quad . \tag{4b}$$

To make the Eqs. (4) a complete set we must add a number of equations relating the fluxes to the primary and to the secondary currents. The analysis to obtain these relationships is carried out in Appendix A. Substitution of the relationship between the fluxes and the currents (A9, A11, A12, A14, A16, A18, A19, and A22) into the Eqs. (4a) and (4b) leads to:

$$L_1 \dot{I}_1 \left[\int_0^d \frac{\ell}{Nd} \dot{J}_{F1}\, x dx\right] + M_{12}\dot{I}_2 + F_{12}\left[\int_0^d \frac{\ell}{d} \dot{J}_{F2}\, x dx\right] + R_1 i_1 = e \quad , \tag{5a}$$

$$L_2 \dot{I}_2 + F_2 \left[\int_0^d \frac{\ell}{d} \dot{J}_{F1}\, x dx\right] + F_B \left[\int_0^{d_B} \frac{\ell}{d_B} \dot{J}_{FB}\, x dx\right] + M_{12}\dot{I}_1 + F_{12}\left[\int_0^d \frac{\ell}{Nd} \dot{J}_{F1}\, x dx\right] + R_2 i_2 = 0 \quad , \tag{5b}$$

which together with the relationships between the driving currents and the eddy currents,

$$-\mu_o x \dot{I}_1 = \eta \frac{\ell}{N} J_{F1}(x) + \mu_o \left[\int_0^x x' \frac{\ell}{N} \dot{J}_{F1}(x')dx' + x\int_x^d \frac{\ell}{N} \dot{J}_{F1}\, dx'\right], \tag{6a}$$

$$-\mu_o x \dot{I}_2 = \eta \ell J_{F2}(x) + \mu_o \left[\int_0^x x' \ell \dot{J}_{F2}(x')dx' + x\int_x^d \ell \dot{J}_{F2}(x')dx'\right] \quad , \tag{6b}$$

$$-\mu_o x \dot{I}_2 = \eta \ell J_{FB}(x) + \mu_o \left[\int_0^x x' \ell \dot{J}_{FB}(x')dx' + x\int_x^{d_B} \ell \dot{J}_{FB}(x')dx'\right] \tag{6c}$$

form the complete circuit equations. The relations (6a) and (6b) between the eddy current density $J_F(x)$ and the primary and secondary currents describe the diffusion of the corresponding fluxes (from the primary and

secondary currents) into a winding; equation (6c) describes the diffusion of the flux from the secondary current into the copper of the Bitter plates. The coefficients of induction L_1, F_1, M_{12}, F_{12}, L_2, F_2, and F_B depend on the dimensions of the transformer and are defined by the relations (A10, A17, A13, A20, A15, A21, and A22). For the dimensions listed in Table I (page 6) these coefficients take on the values listed in Table A in Appendix A.

4. FREQUENCY DEPENDENCE OF THE PARAMETERS ON THE SYSTEM AND EXPERIMENTAL VERIFICATION OF THE MODEL

On the basis of the derived circuit equations we investigate the harmonic behaviour of the transformer and compare the results with measured data of the Alcator transformer.

If a harmonic signal, $e_1 = \hat{e}_1 e^{i\omega t}$, is applied at the primary of the transformer, all quantities will vary harmonically in time. The integral-differential Eqs. (6a), (6b), and (6c), which relate the eddy current densities to the primary and secondary currents are readily solved in this case. Upon differentiating (6a) twice with respect to x, we obtain the simple differential equation:

$$\eta \frac{\ell}{N} \frac{d^2}{dx^2} J_{F1}(x) + i\omega\mu_o \frac{\ell}{N} J_{F1}(x) = 0 \quad . \tag{7}$$

From symmetry considerations it follows that the solution is:

$$\frac{\ell}{N} J_{F1}(x) = C_1 \sinh\left[\frac{1+i}{\delta_s} x\right] \quad , \tag{8}$$

where $\delta_s = \sqrt{2\eta/\mu_o\omega}$ is the skin depth of the copper windings of the primary. The constant C_1 is found upon substitution of Eq. (8) into Eq. (6a), taking x = d:

$$C_1 = \frac{-(1+i)}{\delta_s \cosh\left(\frac{1+i}{\delta_s} d\right)} I_1 \quad .$$

With this solution for J_{F1} we find:

$$\int_0^d \frac{\ell}{Nd} \dot{J}_{F1}(x) x dx = -\left[1 - \frac{\delta_s}{(1+i)d} \tanh\left(\frac{1+i}{\delta_s} d\right)\right] \dot{I}_1 \quad .$$

Similarly for J_{F2} the following relation can be derived:

$$\int_0^d \frac{\ell}{d}\, \dot{J}_{F2}(x)\, x\, dx = -\left[1 - \frac{\delta_s}{(1+i)d} \tanh\left(\frac{1+i}{\delta_s}\, d\right)\right] \dot{I}_2 \quad ,$$

and for J_{FB}:

$$\int_0^{d_B} \frac{\ell}{d_B}\, \dot{J}_{FB}(x)\, x\, dx = -\left[1 - \frac{\delta_s}{(1+i)d_B} \tanh\left(\frac{1+i}{\delta_s}\, d_B\right)\right] \dot{I}_2 \quad .$$

Substitution of these expressions into Eqs. (5a) and (5b) leads to:

$$\begin{aligned} \left[i\omega\tilde{L}_1(\omega) + R_1\right]\hat{i}_1 + i\omega\tilde{M}_{12}\hat{i}_2 &= \hat{e}_1 \quad , \\ \left[i\omega\tilde{L}_2(\omega) + R_2\right]\hat{i}_2 + i\omega\tilde{M}_{12}\hat{i}_1 &= 0 \quad , \end{aligned} \tag{9}$$

where $\tilde{L}_1$, $\tilde{L}_2$, and $\tilde{M}_{12}$ are equal to:

$$\begin{aligned} \tilde{L}_1(\omega) &= L_1 - F_1\alpha(\omega) \quad , \\ \tilde{L}_2(\omega) &= L_2 - F_2\alpha(\omega) - F_B\left[1 - \frac{\delta_s/d_B}{1+i} \tanh \frac{(1+i)d_B}{\delta_s}\right] \quad , \\ \tilde{M}_{12}(\omega) &= M_{12} - F_{12}\alpha(\omega) \quad , \\ \alpha(\omega) &= 1 - \frac{\delta_s/d}{1+i} \tanh \frac{(1+i)d}{\delta_s} \quad . \end{aligned} \tag{10}$$

The real parts of these functions have been plotted in Figs. 5, 6, and 7 as a function of the frequency at room temperature and at LN_2-temperture; for the coefficients L and F we took the calculated values of Table A (Appendix A). Experimental values measured at room temperature are also shown. The overall agreement proves that the model is a good approximation.

Two discrepancies are apparent. The mutual inductance measured to several loops (Fig. 6) around the primary should be the same if there is no return flux; loop 2-I is closely wound on the primary while loop 2-II is at the plasma location. In reality there is a difference: the mutual inductance to 2-II does not change as much with the frequency as predicted. This must be ascribed to a failure of the compensation at higher frequencies due to the change in flux distribution over the cross section of the primary coil. As a consequence a reverse-Foucault-flux arises which is approximately in phase with the original flux and therefore causes an extra induced voltage in the second loop 2-II with

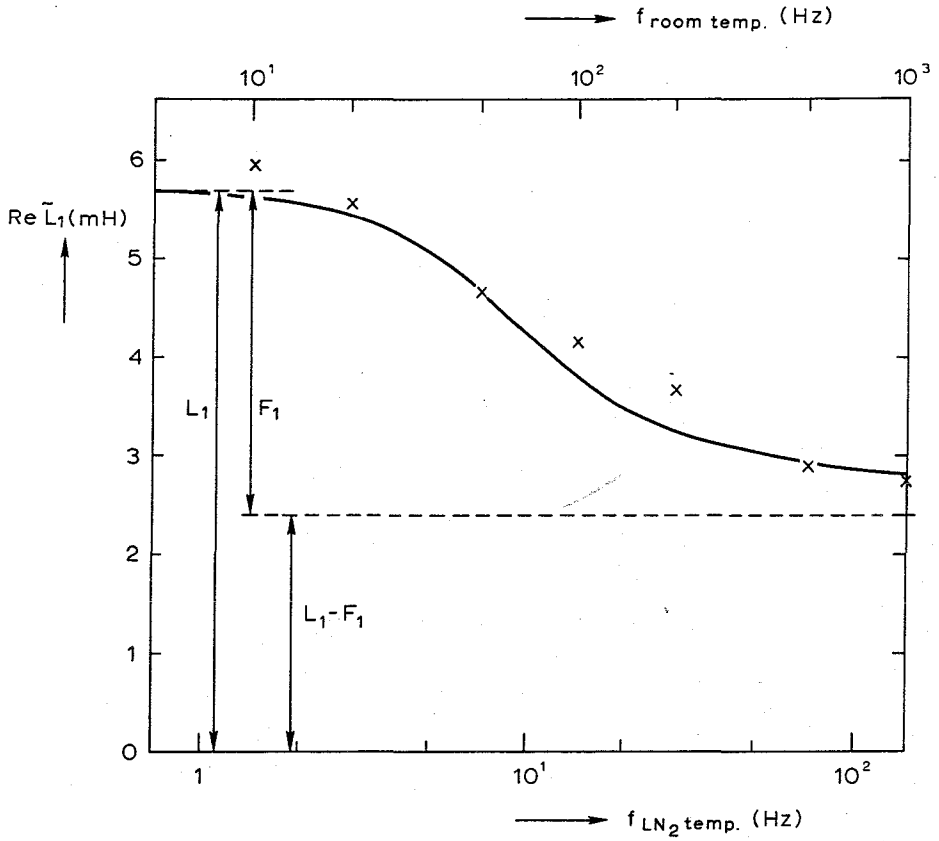

Fig. 5 Primary inductance as a function of the frequency.

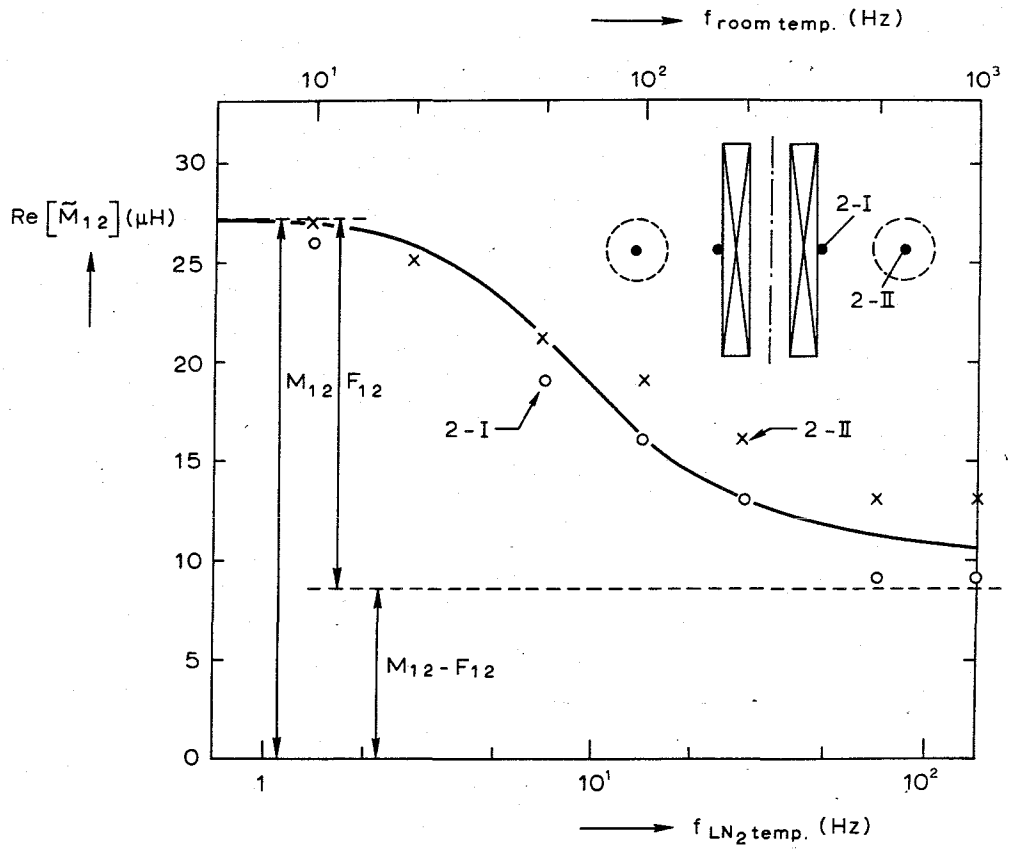

Fig. 6 Mutual inductance as a function of the frequency.

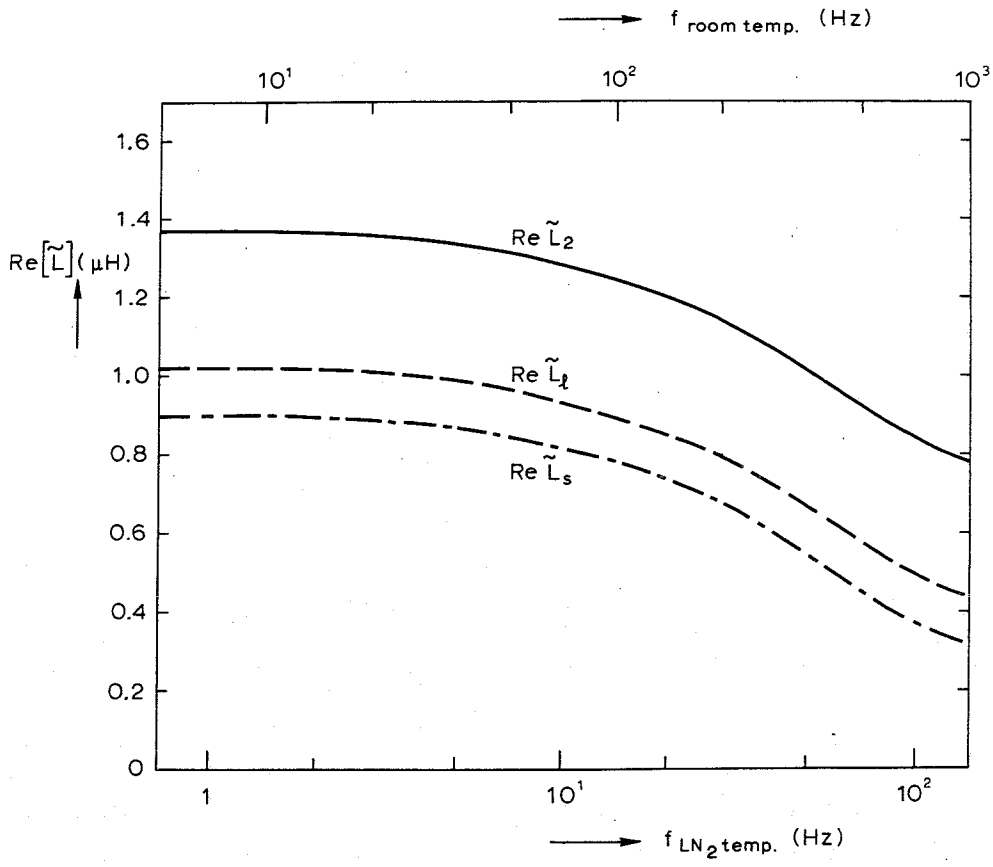

Fig. 7 Plasma (2), shell (s), liner (1) inductances as a function of the frequency.

respect to loop 2-I. This is shown schematically in Fig. 8. This effect implies the existence of a vertical magnetic field attenuated by the copper shell at the plasma location. If this field is tolerable we can numerically introduce this effect by taking $F_{12}/M_{12} = 0.54$ instead of $F_{12}/M_{12} = 0.70$. In general, such a field cannot be tolerated because of force problems, and a dynamic compensation must be designed (F_{12}/M_{12} is then again 0.70). Such a dynamic compensation can be realized by artificially delaying the collapse of flux in the compensation windings[2]. This can be achieved by connecting a resistor parallel to the compensation coils. Figure 9 shows the scheme and the effect of the dynamic compensation.

On the basis of the inductances and resistances appearing in Eqs.(9), we can define the following quality factors:

$$Q_1(\omega) = \frac{\mathrm{Re}\left(\tilde{L}_1(\omega)\right)}{\mathrm{Im}[\tilde{L}_1(\omega) + R_1/\omega]} \quad , \quad Q_2(\omega) = \frac{\mathrm{Re}\left(\tilde{L}_2(\omega)\right)}{\mathrm{Im}[\tilde{L}_2(\omega) + R_2/\omega]} \quad ,$$

$$Q_{12}(\omega) = \frac{\mathrm{Re}\left(\tilde{M}_{12}(\omega)\right)}{\mathrm{Im}[\tilde{M}_{12}(\omega)]} \quad . \qquad (11)$$

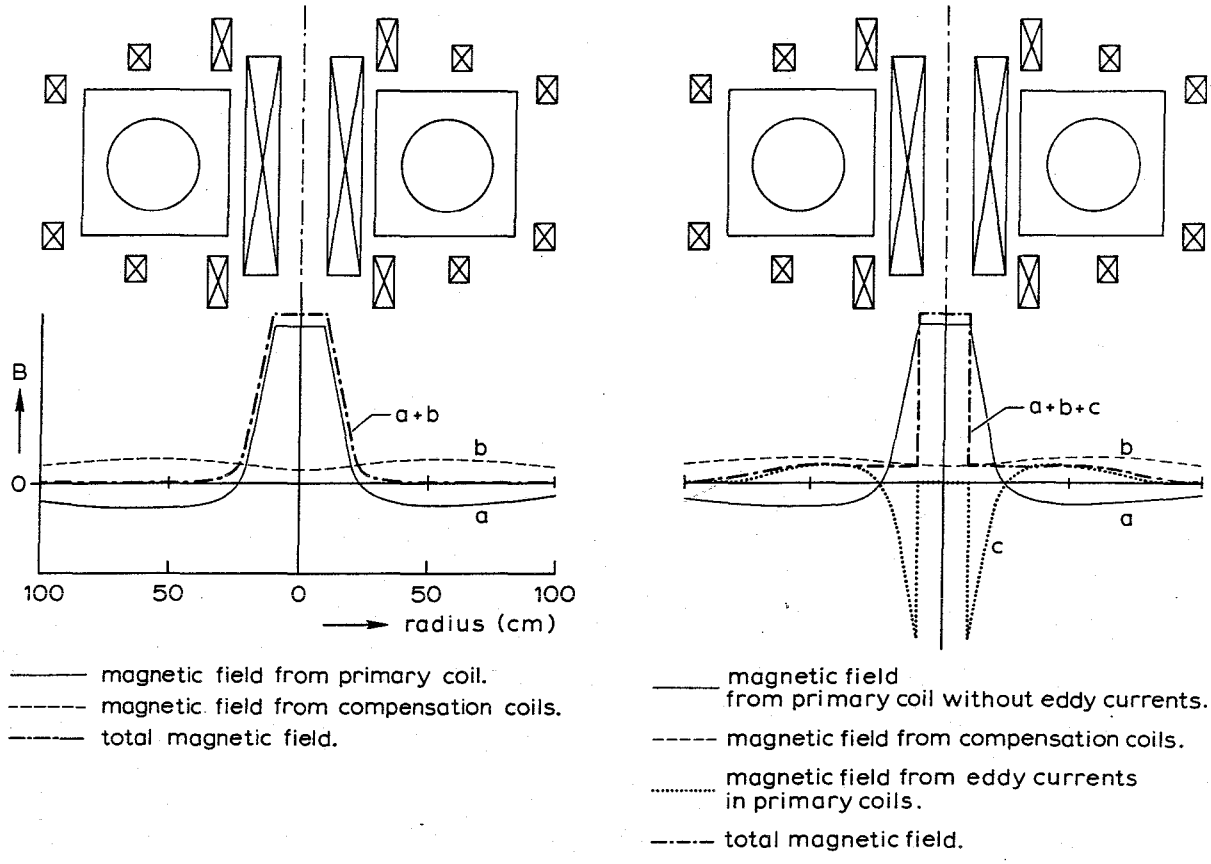

Fig. 8 a. Sketch of magnetic field strength in the absence of eddy currents.
b. Sketch of magnetic field strength with eddy currents (without Bitter magnet).

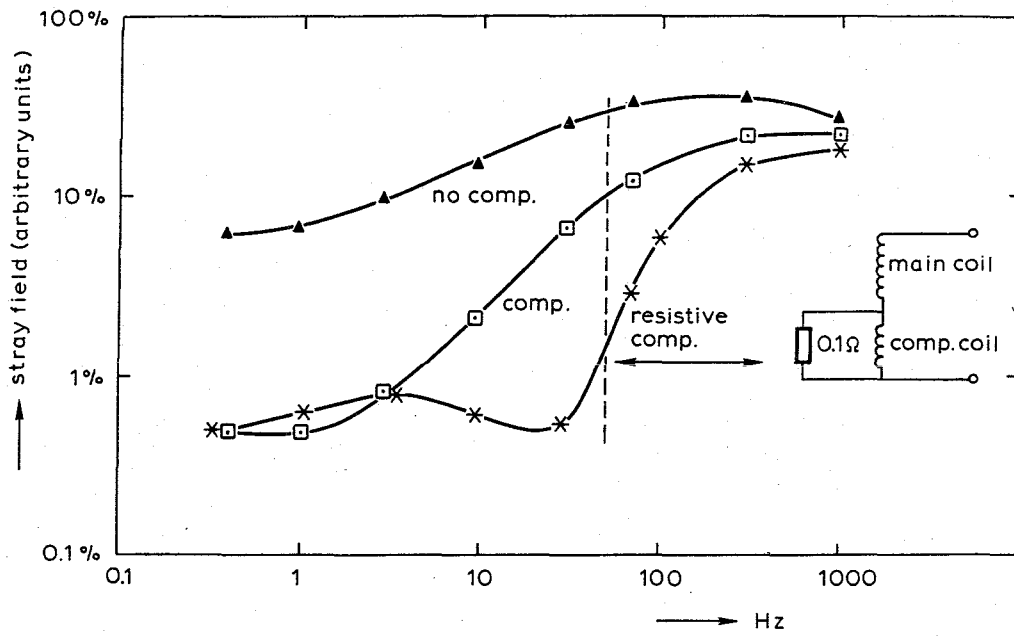

Fig. 9 Vertical magnetic stray field without compensation, with compensation coils, and with resistive compensation [2].

In Fig. 10 a discrepancy between measured and predicted values for these quality factors is apparent. For frequencies above the skin frequency ($\omega_s \equiv 1/\tau_s$) as defined in Eq. (3a), the quality factor should increase with the frequency. Measurements (x,0) show, however, that above that frequency the quality remains close to 3 at least to frequencies of 800 Hz. This may be due to vertical proximity effects between the helical windings of the pancakes. In conclusion we may state that the model describes reasonably well the frequency behaviour of the Alcator transformer.

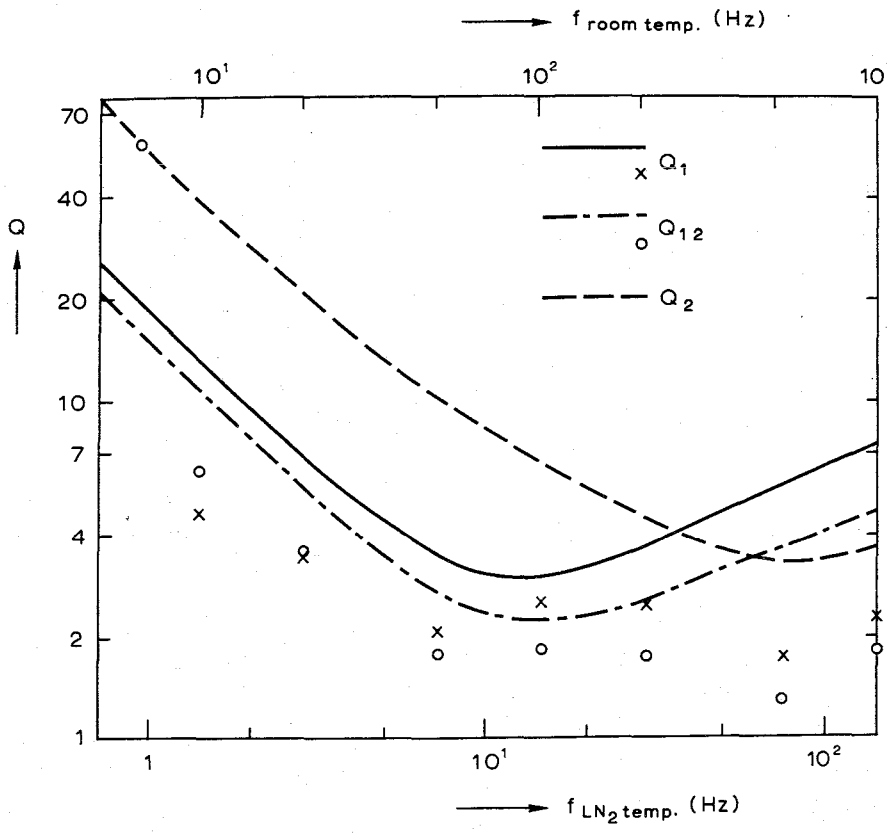

Fig. 10 Quality factor as a function of the frequency.

5. INDUCTIVE HEATING OF THE LINER AND DISCHARGE CLEANING

With the results of the preceding section we can estimate the energy required to heat the liner or to perform repeated discharges at low levels (so called "discharge cleaning"). Both methods are generally employed to improve the quality of the Tokamak discharge; especially the latter method appears to result in an appreciable decrease in the contamination of Tokamak plasmas. As for these two methods the resistance and the inductance of the secondary ($R_2 \simeq 4.7$ mΩ) are comparable, the same treatment applies to both. We shall focus our attention on liner heating but we shall also give results for the case of discharge

cleaning in the absence of the liner. We note, however, that in the case of discharge cleaning the power dissipated in the liner will be approximately equal to the power dissipated in the discharge. Therefore, it would be better to have a higher resistance for the liner.

Several methods can be employed to induce a current in the liner. Consecutively, we shall consider excitation by means of the air-core transformer, of the copper shell, or of the compensation coils. If the liner is heated by means of the primary of the transformer, then Eqs. (9) describe the harmonic behaviour of the system. The total dissipated power, P_{diss}, is equal to:

$$P_{diss} = \frac{1}{2} \mathrm{Re}(\hat{e}_1 \cdot \hat{i}_1^*) = \frac{1}{2} \mathrm{Re} \left[i\omega \tilde{L}_1(\omega) + R_1 - \frac{(i\omega \tilde{M}_{1\ell})^2}{i\omega \tilde{L}_\ell + R_\ell} \right] \hat{i}_1 \hat{i}_1^* \quad .$$

Expressed in terms of the power dissipated in the liner this is (cf. Fig. 11):

$$P_{diss} = \mathrm{Re} \left[i\omega \tilde{L}_1 + R_1 - \frac{(i\omega \tilde{M}_{1\ell})^2}{i\omega \tilde{L}_\ell + R_\ell} \right] \left[\frac{(i\omega \tilde{L}_\ell + R_\ell)(-i\omega \tilde{L}_\ell^* + R_\ell)}{\omega^2 \tilde{M}_{1\ell} \tilde{M}_{1\ell}^*} \right] \frac{P_{liner}}{R_2} . \quad (12)$$

The expressions for $\tilde{L}_\ell$ and $\tilde{M}_{1\ell}$ are obtained from Eqs. (10) by replacing 2 by ℓ. The quantities F_ℓ, $F_{1\ell}$, $M_{1\ell}$ are equal to F_2, F_{12}, and M_{12}, respectively, and L_ℓ is equal to the value given in Eq. (2). The quantities P_{diss}/P_{liner} and $P_{diss}/P_{discharge}$ are sketched in Fig. 11 as func-

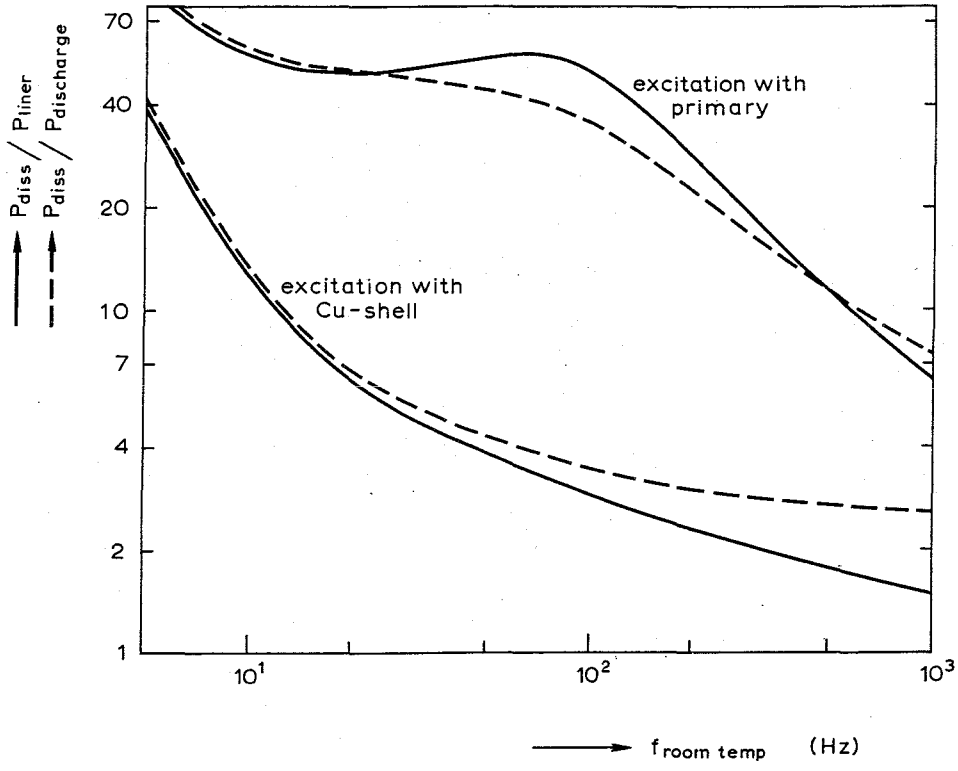

Fig. 11

Dissipated power as a function of frequency. The total dissipated power is normalized to the liner dissipation in the case of liner heating (——) and to the discharge power in the case of discharge cleaning (----).

tions of the frequency. In both curves it is assumed that $R_2 = 4.7$ mΩ and that the operation is done at room temperature ($R_1 = 6.5$ mΩ).

We observe that eddy effects in the primary and the Bitter magnet make the dissipation so excessive that it is impossible to apply this scheme at 60 Hz; this frequency is too low compared to the inverse of the secondary time constant (open transformer) and is too close to the skin frequencies of the copper parts of the machine. At higher frequencies we approach the optimal loading of the transformer ($\omega \sim 1/\tau_2$) and at the same time the Q-factor of the primary increases. Extrapolation of the curve in Fig. 10 would e.g. yield a Q of ~ 5 at 1.5 kHz. Further measurements showed Q's in the order of 6 - 8. This would give rise to a dissipation in the primary which is 5 times the liner dissipation at 1.5 kHz.

If instead we would drive the copper shell, there would be a slight difference between liner and discharge cleaning. In the first case the inductance is lower and consequently the stray inductance between exciting and secondary system would be smaller. Again we will describe the liner heating only. We now assume, that the primary is open so that only eddy currents cause additional dissipation. The following relations hold:

$$\begin{aligned} \hat{e}_s &= i\omega\tilde{L}_s\hat{i}_s + R_s\hat{i}_s + i\omega\tilde{M}_{s\ell}\hat{i}_\ell \\ 0 &= i\omega\tilde{L}_\ell\hat{i}_\ell + R_\ell\hat{i}_\ell + i\omega\tilde{M}_{s\ell}\hat{i}_s \quad , \end{aligned} \tag{13}$$

where $\hat{i}_s$, $\hat{i}_\ell$, $\tilde{L}_s$, R_s, $\tilde{M}_{s\ell}$, $\tilde{L}_\ell$, and R_ℓ are the current in the shell, the current in the liner, the inductance of the shell, the resistance of the shell, the mutual inductance between shell and liner, the liner inductance and resistance, respectively. If we assume that in the considered frequency range the copper shell is a magnetic surface

$$\tilde{M}_{s\ell} = \tilde{L}_s = L_s \left[1 - \frac{F_2}{L_s} \left\{ 1 - \frac{\delta_s}{d(1+i)} \tanh \frac{(1+i)d}{\delta_s} \right\} - \frac{F_B}{L_s} \left\{ 1 - \frac{\delta_s}{d_B(1+i)} \tanh \frac{(1+i)d_B}{\delta_s} \right\} \right]$$

$$L_s = \mu_o R_o \left[\ln \frac{8R_o}{r_s} - 2 \right] \quad . \tag{14}$$

Analogously as in the first case, we can express the total dissipated power in terms of liner power if we replace in Eq. (12) the subscripts $1,\ell$ by s,ℓ. Again P_{diss}/P_{liner} is plotted (Fig. 11) as a function of the frequency. We observe that the power dissipation at 60 Hz is remarkably reduced, though there may still be too much dissipation in the copper

shell. Again excitation at a higher frequency is better.

A third possible means of excitation is to make use of the compensation coils, which are located outside the Bitter magnets. This case is estimated to be intermediate between the two foregoing methods of excitation. From a practical point of view the last method may be the most preferable one as the compensation coils are water-cooled.

6. TIME BEHAVIOUR OF THE PLASMA CURRENT

In a Tokamak there are several ways to operate the transformer. If the required flux is not too large and an iron yoke can be used, the initial flux can be taken zero. In this type of operation the stray fields from the core are initially zero and the plasma current is limited by the saturation of the core. For larger plasma currents it is advantageous to start with a maximum reversed flux and drive the transformer until the flux reaches the maximum possible value ("double-swing" technique); in this case there are stray fields but the forces will be smaller. An aircore transformer can be discharged in the same way but has the disadvantage that the primary flux decays with its own time constant after the swing. This means that one must take precautions to make this time constant sufficiently long. In the Alcator experiment, this type of operation is not necessary and the flux change is obtained by the decay of the primary current to zero. At the beginning of the actual discharge the primary current has thus its maximum value and the electric field driving the plasma current is induced by rapidly decreasing the primary current. The rate of decrease, which determines the magnitude of the induced electric field, depends on the size of the resistor placed across the primary [1].

In this section we analyse the time behaviour of the plasma current in our model. This behaviour is described by the circuit equations if we add the initial conditions

$$I_1(t=0) \equiv I_o \quad , \quad I_2(t=0) = 0 \quad , \tag{15}$$

and take R_1 to be the sum of the D.C. resistance of the primary and the resistance across the primary. In order to be able to point out the effect of the eddy currents we first consider the time behaviour of the plasma current in the absence of eddy currents.

6a. Time behaviour of the plasma current without eddy currents in the primary and in the Bitter magnet

The analysis of this simple case will enable us later to

understand the effect of the eddy currents. The circuit equations describing the behaviour of the currents in this simplified model are:

$$L_1 \frac{dI_1}{dt} + R_1 I_1 + M_{12} \frac{dI_2}{dt} = 0 \quad ,$$
$$L_2 \frac{dI_2}{dt} + R_2 I_2 + M_{12} \frac{dI_1}{dt} = 0 \quad . \tag{16}$$

With the initial conditions (15) the Laplace transforms of these equations are:

$$(1 + p\tau_1) i_{1p} + p \frac{M_{12}}{R_1} i_{2p} = I_o \tau_1 \quad ,$$
$$(1 + p\tau_2) i_{2p} + p \frac{M_{12}}{R_2} i_{1p} = I_o \frac{M_{12}}{R_2} \quad , \tag{17}$$

and one finds, using the usual definitions for the coupling factor $k^2 = M_{12}^2/L_1L_2$ and the primary and secondary time constants $\tau_1 = L_1/R_1$ and $\tau_2 = L_2/R_2$

$$i_{1p} = \frac{[(1 + p\tau_2)\tau_1 - pk^2\tau_1\tau_2]}{[(1 + p\tau_1)(1 + p\tau_2) - p^2k^2\tau_1\tau_2]} I_o \quad ,$$
$$i_{2p} = \frac{M_{12}\tau_2}{L_2[(1 + p\tau_1)(1 + p\tau_2) - p^2k^2\tau_1\tau_2]} I_o \quad . \tag{18}$$

The roots of the denominators of i_{1p} and i_{2p} are ($p_I = -1/\tau_I$, $p_{II} = -1/\tau_{II}$):

$$\tau_{I,II} = \frac{\tau_1 + \tau_2}{2} \mp \sqrt{\left(\frac{\tau_2 - \tau_1}{2}\right)^2 + k^2\tau_1\tau_2} \quad . \tag{19}$$

(For a weakly coupled transformer the time constants τ_I and τ_{II} are close to τ_1 and τ_2.)
When we take the inverse Laplace transform the currents are found to be:

$$\frac{I_1(t)}{I_o} = \frac{1}{\tau_{II} - \tau_I} \left[\left(\tau_1 - \tau_I\right) e^{-t/\tau_{II}} + \left(\tau_{II} - \tau_1\right) e^{-t/\tau_I}\right] \simeq e^{-t/\tau_I} \quad , \tag{20}$$

$$\frac{I_2(t)}{I_o} = \frac{M_{12}}{L_2} \frac{e^{-t/\tau_{II}} - e^{-t/\tau_I}}{(\tau_{II} - \tau_I)/\tau_2} \simeq \frac{M_{12}}{L_2} \frac{e^{-t/\tau_2} - e^{-t/\tau_1}}{1 - \tau_1/\tau_2} \quad . \tag{21}$$

These results are shown in all figures by the label NF (= Non-Foucault). The secondary current is maximum when $dI_2/dt = 0$, i.e. at the time:

$$t_{max} = \frac{\tau_I}{1 - \tau_I/\tau_{II}} \ln \frac{\tau_{II}}{\tau_I} \quad , \tag{22}$$

and the magnitude is:

$$\frac{I_{2max}}{I_o} = \frac{M_{12}}{L_2} \frac{e^{-t_{max}/\tau_{II}} - e^{-t_{max}/\tau_I}}{(\tau_{II} - \tau_I)/\tau_2} \quad . \tag{23}$$

Later on we shall show that with any Foucault effect this maximum is lowered. Note that the time at which the maximum occurs is proportional to τ_I and only weakly dependent on the secondary time constant τ_{II}. In case $\tau_{II} \gg \tau_I$ with $\tau_I \simeq \tau_1$ and $\tau_{II} \simeq \tau_2$ we find:

$$t_{max} \simeq \tau_1 \ln \frac{\tau_2}{\tau_1} \quad , \tag{24}$$

and

$$\frac{I_{2max}}{I_o} \simeq \frac{M_{12}}{L_2} \left[\tau_1/\tau_2\right]^{\tau_1/\tau_2} \quad . \tag{25}$$

In Figs. 12a and 12b, the results (22) and (23) are compared with measured data. In the absence of the Bitter magnet we find that the simple results (22) and (23) are applicable to a primary time constant long compared to the skin-time constant. If the primary time constant approaches the skin time then we obtain larger values for t_{max} and lower values for I_{2max}/I_o than predicted. This is, of course, due to the Foucault effect in the primary windings. Figure 12b suggests that the rise time of the plasma current is larger than 3 msec at room temperature and larger than 17 msec at 90 K.

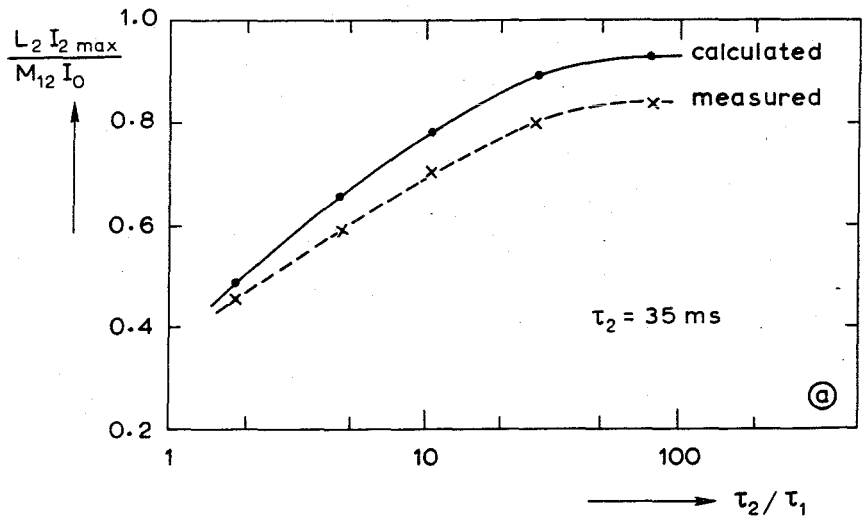

Fig. 12a

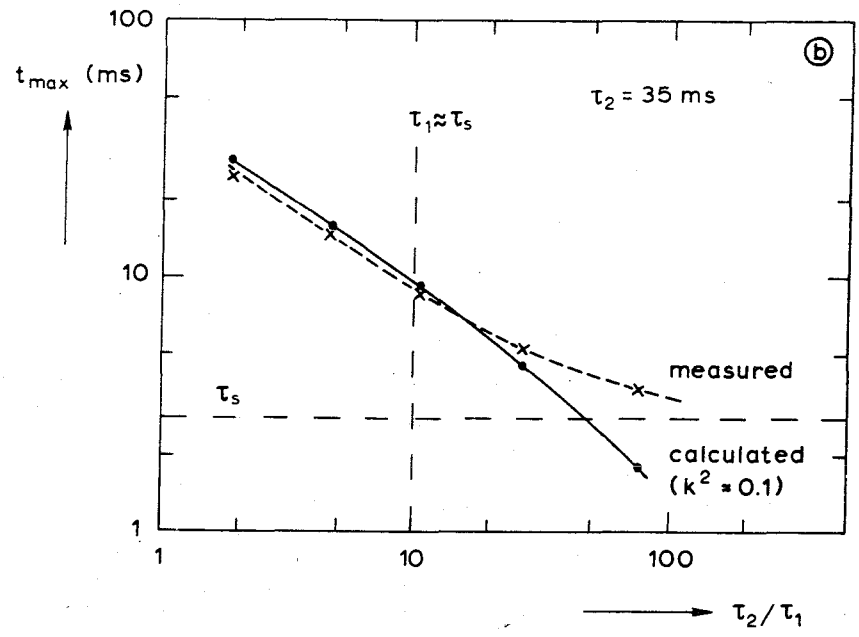

Fig. 12a and b Maximum plasma current and t_{max} as a function of τ_2/τ_1. Experimental data are obtained in the absence of the Bitter magnet; the effect of eddy currents is not taken into account in the calculated values.

6b. Time behaviour of the plasma current with eddy currents in the primary and in the Bitter magnet

With the effect of the eddy currents the time behaviour of the model is described by the Eqs. (5) and (6) and the boundary conditions:

$$I_1(t=0) = I_o \quad , \quad I_2(t=0) = I_{F1}(t=0) = I_{F2}(t=0) = I_{FB}(t=0) = 0.$$

To solve this system we proceed as above, i.e. we take the Laplace transforms of all currents. The equations that these Laplace-transformed currents satisfy are:

$$L_1(pI_{1p} - I_o) + F_1 p\left[\int_0^d \frac{\ell}{Nd} J_{F1p} x'dx'\right] + M_{12} pI_{2p} + F_{12} p\left[\int_0^d \frac{\ell}{d} J_{F2p} x'dx'\right] + R_1 I_{1p} = 0, \tag{26a}$$

$$L_2(pI_{2p}) + F_2 p\left[\int_0^d \frac{\ell}{d} J_{F2p} x'dx'\right] + M_{12}(pI_{1p} - I_o) + F_B p \int_0^{d_B} \frac{\ell}{d_B} I_{FBp} x'dx' +$$

$$+ F_{12} p\left[\int_0^d \frac{\ell}{Nd} J_{F1p} x'dx'\right] + R_2 I_{2p} = 0 \quad , \tag{26b}$$

$$- \mu_o x(pI_{2p}) = \eta \ell J_{F2p} + \mu_o \int_0^x x' p\ell J_{F2p}(x')dx' + \mu_o x \int_x^d p\ell J_{F2p}(x')dx' \quad , \tag{27a}$$

$$- \mu_o x(pI_{1p} - I_o) = \eta J_{F1p} \frac{\ell}{N} + \mu_o \int_0^x x' p \frac{\ell}{N} J_{F1p}(x')dx' + \mu_o x \int_x^d p \frac{\ell}{N} J_{F1p}(x')dx', \tag{27b}$$

$$- \mu_o x p I_{2p} = \eta \ell J_{FBp} + \mu_o \int_0^x x' p\ell J_{FBp}(x')dx' + \mu_o x \int_x^{d_B} p\ell J_{FBp}(x')dx' \quad . \tag{27c}$$

We express first the Laplace transforms of the eddy current densities J_{F1p}, J_{F2p}, and J_{FBp} in terms of the Laplace transforms of the primary and the secondary currents (I_{1p}, I_{2p}). These transformations are similar to the Fourier transformations in Section 4:

$$\begin{aligned}
\frac{p}{d} \int_0^d \frac{\ell}{N} J_{F1p} x'dx' &= -(pI_{1p} - I_o)\left[1 - \sqrt{\frac{1}{2p\tau_s}} \tanh \sqrt{2p\tau_s}\right] \quad , \\
\frac{p}{d} \int_0^d \ell J_{F2p} x'dx' &= - pI_{2p}\left[1 - \sqrt{\frac{1}{2p\tau_s}} \tanh \sqrt{2p\tau_s}\right] \quad , \\
\frac{p}{d_B} \int_0^{d_B} \ell J_{FBp} x'dx' &= - pI_{2p}\left[1 - \sqrt{\frac{1}{2p\tau_B}} \tanh \sqrt{2p\tau_B}\right] \quad .
\end{aligned} \tag{28}$$

The time constants τ_s and τ_B are defined in Eqs. (3a) and (3b). With the help of these expressions the Eqs. (26a) and (26b) can be written in the same form as Eqs. (17):

$$\begin{aligned}
(1 + p\tilde{\tau}_1)I_{1p} + p \frac{\tilde{M}_{12}}{R_1} I_{2p} &= \tilde{\tau}_1 I_o \quad , \\
(1 + p\tilde{\tau}_2)I_{2p} + p \frac{\tilde{M}_{12}}{R_2} I_{1p} &= \frac{\tilde{M}_{12} I_o}{R_2} \quad ,
\end{aligned} \tag{29}$$

where

$$\tilde{\tau}_1 = \frac{L_1}{R_1} - \frac{F_1}{R_1}\left[1 - \sqrt{\frac{1}{2p\tau_s}} \tanh \sqrt{2p\tau_s}\right] \quad ,$$

$$\tilde{\tau}_2 = \frac{L_2}{R_2} - \frac{F_2}{R_2}\left[1 - \sqrt{\frac{1}{2p\tau_s}} \tanh \sqrt{2p\tau_s}\right] - \frac{F_B}{R_2}\left[1 - \sqrt{\frac{1}{2p\tau_B}} \tanh \sqrt{2pt_B}\right],$$

$$\tilde{M}_{12} = M_{12} - F_{12}\left[1 - \sqrt{\frac{1}{2p\tau_s}}\tanh\sqrt{2p\tau_s}\right] \quad . \tag{30}$$

Hence, the Laplace transforms of the primary and secondary currents are:

$$\frac{I_{1p}}{I_o} = \frac{(1+p\tilde{\tau}_2)\tilde{\tau}_1 - p\tilde{M}_{12}^2/R_1R_2}{(1+p\tilde{\tau}_1)(1+p\tilde{\tau}_2) - p^2\tilde{M}_{12}^2/R_1R_2} = \frac{1}{p} - \frac{1}{pD} - \frac{\tilde{\tau}_2}{D} \quad ,$$

$$\frac{I_{2p}}{I_o} = \frac{\tilde{M}_{12}/R_2}{(1+p\tilde{\tau}_1)(1+p\tilde{\tau}_2) - p^2\tilde{M}_{12}^2/R_1R_2} \quad , \tag{31}$$

where

$$D = (1+p\tilde{\tau}_1)(1+p\tilde{\tau}_2) - p^2\frac{\tilde{M}_{12}^2}{R_1R_2} \quad .$$

If we denote the roots of D by p_n, the inverse Laplace transforms of I_{1p} and I_{2p} in the real time domain are:

$$\frac{I_1(t)}{I_o} = -\sum_{n=1}^{\infty}\frac{e^{p_n t}(1+p_n\tilde{\tau}_2)}{p_n D'(p_n)} \quad ,$$

$$\frac{I_2(t)}{I_o} = \frac{1}{R_2}\sum_{n=1}^{\infty}\frac{\tilde{M}_{12}(p_n)}{D'(p_n)}e^{p_n t} \quad , \tag{32}$$

where

$$D'(p_n) = \left(\frac{dD}{dp}\right)_{p=p_n} \quad .$$

In figure 13a the plasma current is shown as a function of time (normalized to the primary time constant τ_1) for some characteristic cases, cf. Table III.

TABLE III

τ_2/τ_1	4	16	64	16
τ_s/τ_1	0 (NF); 0.25; 1; 4	0 (NF); 0.25; 1; 4	0 (NF); 1; 4	1
τ_B/τ_s	0.16	0.16	0.16	0; 0.16; 1.0
	Figure 13a			Fig. 13b (I_2) and Fig. 13c (dI_2/dt)

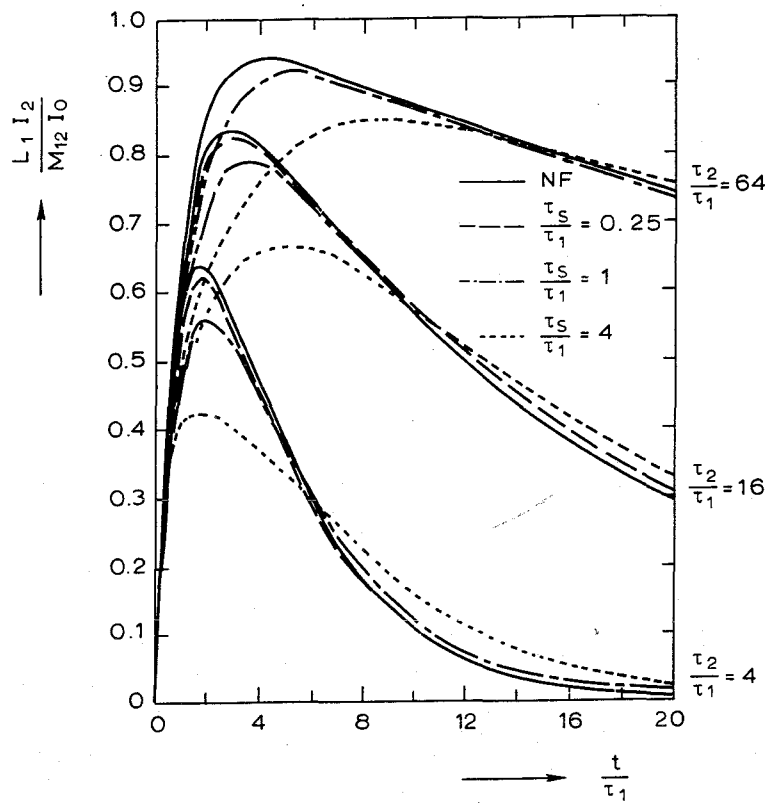

Fig. 13a Normalized plasma current as a function of normalized time (t/τ_1) for various values of τ_2/τ_1 and τ_s/τ_1; (NF) = without eddy currents ($\tau_s/\tau_1 = 0$).

The curves can be compared with those labelled NF (Non-Foucault), for which eddy currents have been neglected. Comparison of the curves for increasing values of τ_s/τ_1 at a fixed value of τ_2/τ_1 and τ_B/τ_s (0.16) shows that the eddy currents in the aircore transformer lower the maximum plasma current by an increasing amount, especially if the secondary time constant is small. A reduction of 8% must be anticipated in the case of Alcator ($\tau_1 \sim \tau_s \sim 17$ msec, $\tau_B \sim 3$ msec, $\tau_2 \sim 270$ msec). Naturally, this reduction is large when the primary time constant τ_1 is small compared to the skin-time constant τ_s; for small skin-time constants ($\tau_s/\tau_1 = 0.25$) the effect is very small. Note, that a factor of 4 in the skin-time constant corresponds only to a factor of 2 in the thickness of the lamination (cf. Eqs. (3a), (3b)).

In Fig. 13b the net effect of the eddy currents in the Bitter magnet is clearly demonstrated by comparison of the plasma currents for $\tau_B/\tau_s = 0$; 0.16 and 1.0 for fixed values of $\tau_s/\tau_1 = 1$ and $\tau_2/\tau_1 = 16$; $\tau_B/\tau_s = 0.16$ corresponds to the average width of the tapered Alcator Bitter plates. The eddy currents in the Bitter plates affect predominantly the initial current rise and have little influence on the current maximum. The initial current rise is steepened (cf. Fig. 13c for dI_2/dt). This effect can be made plausible as follows. An appreciable

part of the volume between plasma and primary is filled with copper, that of the aircore transformer itself and of the Bitter magnet. On a time scale short compared to the skin-time constants eddy currents prevent the magnetic flux from decaying in the copper.

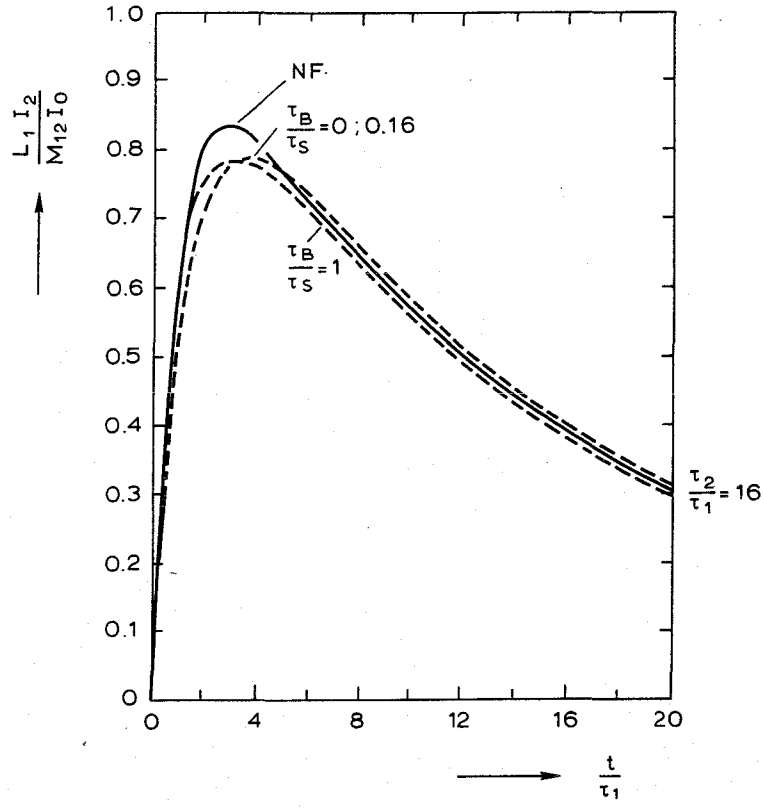

Fig. 13b Normalized plasma current as a function of normalized time (t/τ_1) for various time constants of the Bitter magnet: τ_B/τ_s = 0, 0.16, 1, and for fixed values of the normalized time constants τ_2/τ_1 and τ_s/τ_1.

This leads to a reduction of the secondary (plasma) inductance from L_2 to

$$L_2 \cdot \left(1 - \frac{F_2}{L_2} - \frac{F_B}{L_2}\right)$$

and to a larger coupling factor

$$k^2 \cdot \frac{(1 - F_{12}/M_{12})}{\left(1 - \frac{F_1}{L_1}\right)\left(1 - \frac{F_2}{L_2} - \frac{F_B}{L_2}\right)} = k^2 f_k \quad . \tag{33}$$

As a consequence the plasma current increases faster since approximately (weakly coupled transformer)

$$L_2 \frac{dI_2}{dt} \simeq M_{12} \frac{dI_1}{dt} \simeq M_{12} I_o e^{-t/\tau_1} \quad . \tag{34}$$

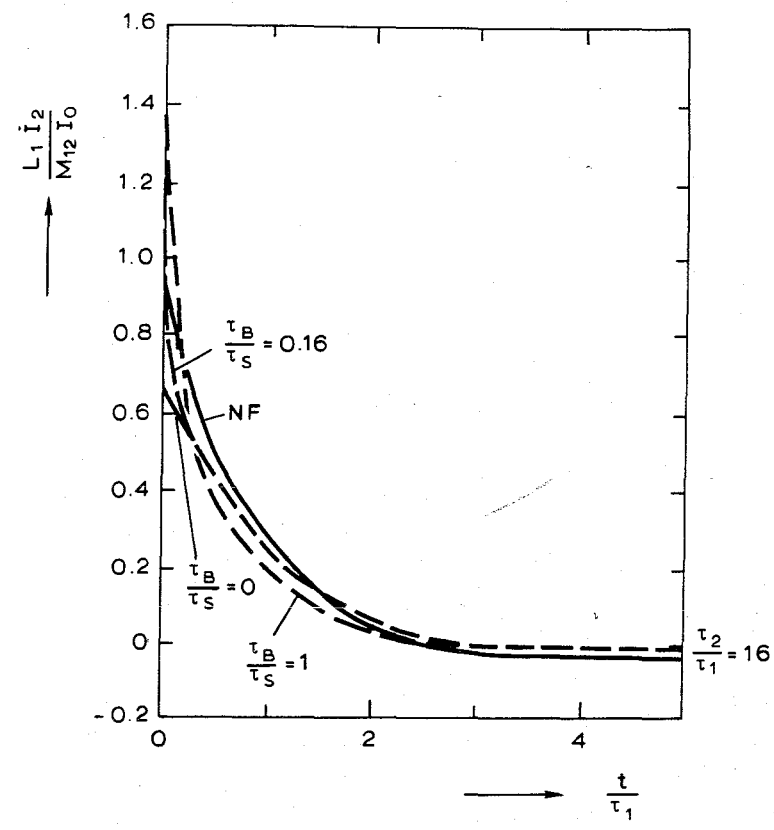

Fig. 13c The normalized time derivative of the plasma current as a function of normalized time for the same parameters as in Fig. 13b.

In the present discussion (a constant plasma resistance) this effect leads to a faster increase of the plasma current and therefore to a favourable increase of the ohmic heating during the ionization phase. However, in a more realistic description, the time dependence of the plasma resistance (which is an extremely rapid varying function of time in the beginning of the discharge) must be accounted for. A complete analysis should include a nonlinear differential equation for the plasma current coupled to the diffusion equations for the eddy currents and to the equations for the energy and the particle balances of the plasma.

In Appendix C we have investigated the effect of a time-dependent resistance on the plasma current in the initial phase of the discharge on the basis of a number of simplifying assumptions. In particular, particle and energy losses are neglected and it is assumed that at any time sufficient power is available for ionization and excitation. In this simplified model, the equation for the plasma current is decoupled from the particle and energy balances: the resistance is a known function of time and does not depend on plasma current.

Two phases are distinguished in the initial stage: phase A where electron-neutral collisions dominate, and phase B where electron-

ion collisions are more frequent. For both phases we evaluated the *additional* reduction (above the reduction caused by eddy currents) of the plasma current, both without (C.19, C.35) and with eddy currents ($C.19^F$, $C.35^F$). The estimated reduction is small for Alcator for long primary time constants (a few per cent); inclusion of the eddy currents in the model leads to an increase of this reduction by a factor of f_k which for Alcator is in the order of 2 (cf. Eqs. $C.19^F$, $C.35^F$, and Eq. 33). The eddy currents in the Bitter magnet are now found to play a dominant role in contrast with their net effect in the case of a constant low plasma resistance; that reduction of the current was shown to be mainly caused by eddy currents in the primary.

As stated above the plasma current is only slightly reduced if the primary time constant (τ_1) is long compared to the duration of the ionization phase Δt. Since the reduction is proportional to $\Delta t/\tau_1$, the ionization phase should be as short as possible. Consequently, it is of importance to start with a good preionization, in particular for devices with relatively small primary time constants. Additional electron heating e.g., hf-heating will also be advantageous. A higher electron temperature will lead to a shorter ionization phase and the additional power input will make it easier to fulfil the energy requirement. In the case of Alcator (with a larger τ_1) a good preionization should not be essential, at least in view of this simple analysis.

The analysis is based on the assumption that the power input due to ohmic heating is, at any time, sufficient to supply the required power to dissociate and ionize the gas. It can be made plausible that this is not difficult to meet in phase A. In phase B, however, it is difficult to fulfil this requirement (C.37) simultaneously with the requirement that the electric field strength should remain below the Dreicer limit (C.39). In practice the power requirement may not impose a serious problem because the drift velocity of the electrons will be well above the ion-acoustic speed. Hence, ion-acoustic turbulence can be anticipated to occur and the corresponding anomalously high resistance may lead to a sufficient increase of the power input.

It should be emphasized that the model must be regarded as optimistic because particle influx, the influence of impurities and losses are neglected. All these assumptions may well be invalidated, in particular during phase B and consequently, the reduction of the plasma current due to the time dependence of the resistance is underestimated in this model.

7. CONCLUSIONS

a) Eddy currents in the primary of the aircore transformer lower the attainable plasma current by a considerable percentage and introduce compensation problems for the vertical magnetic field. These eddy currents can be avoided by laminating the primary windings such that the skin-time constant τ_s is smaller than the primary time constant τ_1.

b) Eddy currents in copper structures between the primary and the plasma, e.g. Bitter magnet, enhance the rate of rise of the plasma current. The influence on the maximum attainable plasma current is small provided that the skin-time constant of the Bitter magnet (τ_B) is not too long.

c) The reduction of attainable plasma current due to the time dependence of the plasma resistance is small for long primary time constants. A good preionization and electron heating minimize this reduction.

d) Eddy currents in the primary windings and Bitter magnet enlarge the reduction of the attainable plasma current if both τ_s and τ_B are longer than the duration of the initial phase.

e) The requirement that the ohmic heating power should be sufficient at any time to supply the ionization and excitation losses is difficult to meet if the electric field strength is supposed to be below the Dreicer limit. However, anomalous resistance due to ion-acoustic turbulence may lead to enhanced heating.

The simplistic analysis of Appendix C clearly indicates the need for a more detailed knowledge of the initial phase of the discharge. Precise measurements of T_e and n_e during the build-up of the plasma current would be of great help in establishing more elaborate treatments and should indicate which additional effects have to be included in the analysis.

ACKNOWLEDGEMENTS

It is a pleasure to thank the members of the Alcator team for the many useful and stimulating discussions. The authors acknowledge in particular the discussions with Dr. B. Coppi, Dr. B. Montgomery Dr. L.Th.M. Ornstein, and Dr. R. Taylor. The skilful assistance of Mr. C.J.A. Hugenholtz with some of the numerical calculations and measurements is gratefully acknowledged.

This work was performed as part of the research programme of the association agreement of Euratom and the "Stichting voor Fundamenteel onderzoek der Materie" (FOM) with financial support from the "Nederlandse Organisatie voor Zuiver-Wetenschappelijk Onderzoek" (ZWO) and Euratom.

REFERENCES

1. Quarterly Progress Report October - December 1970, MIT, Francis Bitter Magnet Laboratory, Cambridge (Mass.).
2. D.C. Schram et al., Proc. 7th Symposium on Fusion Technology, Grenoble, 1972, p. 319.
3. J.N. Di Marco and S.E. Segre, Private Communication, 1972.
4. P. Laborie et al., Electronic cross sections and macroscopic coefficients, 1-hydrogen and rare gases, Dunod, 1968.
5. M. Abramowitz and I.A. Stegun, Handbook of Mathematical Functions, National Bureau of Standards, 1964.

A P P E N D I X A

CIRCUIT EQUATIONS FOR THE PRIMARY AND THE SECONDARY OF THE TRANSFORMER

The circuit equations derived in Section 3 contain several fluxes. Below we shall derive the relationships between these fluxes and the primary and secondary currents (e.g. $\phi_{11} = L_1 I_1$). However, we shall first derive relationships between the eddy currents and the primary and secondary currents. To arrive at these we have to consider in some detail the diffusion of a magnetic field out of a copper winding of a pancake, or a plate of the Bitter coil. Let us first consider the relation between I_{F2} and I_2.

A change in the secondary current induces a magnetic field change

$$\dot{B}_2 = \mu_o \frac{\dot{I}_2}{\ell} \quad , \tag{A.1}$$

at the location of the primary. This flux change causes eddy currents to flow in the copper windings of the primary. To determine these currents we consider a closed loop of thickness dx in the m-th winding of a pancake at a distance ± x from the centre line of this winding, r_m. The induced voltage in this loop is (cf. Fig. A):

$$2x \; 2\pi r_m \dot{B}_2 = 2x \; 2\pi r_m \mu_o \frac{\dot{I}_2}{\ell} \quad . \tag{A.2}$$

The eddy currents in the m-th winding driven by this flux change are a function of x. The total voltage they induce in the loop under consideration is:

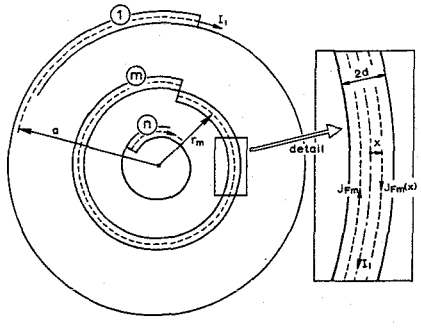

Fig. A Cross section of one pancake and detail.

$$\mu_o 2\pi r_m \left[\int_0^x 2x' \dot{J}_{F2}(x')dx' + 2x \int_x^d \dot{J}_{F2}(x')dx' \right] \quad . \tag{A.3}$$

Since the sum of the induced voltages must be equal to the resistive voltage drop we arrive at the equation (dividing by $4\pi r_m$):

$$- \mu_o \frac{x\dot{I}_2}{\ell} = \eta \dot{J}_{F2}(x) + \mu_o \int_0^x x' \dot{J}_{F2}(x')dx' + \mu_o x \int_x^d \dot{J}_{F2}(x')dx' \quad . \tag{A.4}$$

The derivation of the relationship between I_{F1} and I_1 is similar to the one just derived, except that the source term - the magnetic flux variation - now depends on m, the label of the winding. The flux increases with m (the outer winding being numbered 1). If we assume B to be constant over one winding and equal to the value in the middle of the winding the flux change caused by dI_1/dt is

$$2x \; 2\pi r_m \mu_o \frac{N(m - \tfrac{1}{2})\dot{I}_1}{\ell} \quad . \tag{A.5}$$

The eddy current in the m-th winding will thus also depend on m through $m - \frac{1}{2}$. Therefore, we introduce an eddy current density which is independent of m:

$$J_{F1} = \frac{J_{Fm}}{m - \frac{1}{2}} \quad , \tag{A.6}$$

where J_{Fm} is the eddy current density in the m-th winding. Proceeding in the same manner as in the derivation of Eq. (A.4) we obtain for J_{F1} the equation:

$$- \mu_o x \dot{I}_1 = \eta J_{F1}(x) \frac{\ell}{N} + \mu_o \left[\int_0^x x' \frac{\ell}{N} \dot{J}_{F1}(x')dx' + x \int_x^d \frac{\ell}{N} \dot{J}_{F1}dx' \right] \quad . \tag{A.7}$$

Analogously, for the eddy current in the Bitter magnet we find

$$- \mu_o x \dot{I}_2 = \eta J_{FB}(x)\ell + \mu_o \int_0^x x' \dot{J}_{FB}(x')\ell dx' + \mu_o x \int_x^{d_B} \ell \dot{J}_{FB}(x')dx' . \tag{A.8}$$

The Eqs. (A.4), (A.7), and (A.8) describe the relationships between the eddy currents and the primary and secondary currents. We considered these relations first, because the flux ϕ_{11F}, occurring in Eq. (4) is most easily expressed in terms of I_{F1} (Eq. (A.16)), whose introduction

occurred here naturally.

To complete the circuit equations we still need relationships between the fluxes and the currents, i.e. the coefficients of induction. To keep the calculation general we take the number of windings in a pancake equal to n and the total number of pancakes equal to N. To obtain the primary inductance we sum the induced voltage in each winding. The induced voltage in the m-th winding of the M-th pancake, due to the primary current (which flows through all the windings of the primary) is:

$$- \left(\frac{d\phi_{11}}{dt}\right)_{m,M} = - \mu_o \frac{N}{\ell} \left[\sum_{s=m}^{n} \pi (a - 2sd)^2 + (m - \tfrac{1}{2}) \pi (a - 2md)^2 \right] \frac{dI_1}{dt} \ .$$

Summation over all n-windings of the M-th pancake and over all N-pancakes yields a total induced voltage of:

$$- \frac{d\phi_{11}}{dt} = - \mu_o \frac{N^2}{\ell} \sum_{m=1}^{n} \left[\sum_{s=m}^{n} \pi (a - 2sd)^2 + (m - \tfrac{1}{2}) \pi (a - 2md)^2 \right] \frac{dI_1}{dt}$$

$$= - \mu_o \frac{N^2}{\ell} n^2 \pi a^2 \sum_{m=1}^{n} \frac{(2m - 1)(a - 2md)^2}{n^2 a^2} \frac{dI_1}{dt} \equiv - L_1 \frac{dI_1}{dt} \quad . \qquad (A.9)$$

Here L_1 is the coefficient of self-inductance of the primary coil in the absence of eddy currents (i.e., at zero frequency):

$$L_1 = \mu_o \frac{N^2 n^2 \pi a^2}{\ell} \sum_{m=1}^{n} \frac{(2m - 1)(a - 2md)^2}{n^2 a^2} \simeq 5.70 \text{ mH} \quad . \qquad (A.10)$$

Analogously we find:

$$\frac{d\phi_{12}}{dt} = \mu_o \frac{N}{\ell} \sum_{m=1}^{n} \pi (a - 2md)^2 \frac{dI_2}{dt} \equiv M_{12} \frac{dI_2}{dt} \quad , \qquad (A.11)$$

$$\frac{d\phi_{21}}{dt} = \mu_o \frac{N}{\ell} \sum_{m=1}^{n} \pi (a - 2md)^2 \frac{dI_1}{dt} \equiv M_{12} \frac{dI_1}{dt} \quad . \qquad (A.12)$$

$M_{12} = M_{21}$ is the mutual inductance between primary and the plasma winding at zero frequency:

$$M_{12} = \mu_o \frac{Nn\pi a^2}{\ell} \sum_{m=1}^{n} \frac{(a - 2md)^2}{na^2} \simeq 27.2 \ \mu\text{H} \quad . \qquad (A.13)$$

Finally, the inductance of the plasma at low frequencies in our approximation is:

$$\frac{d\phi_{22}}{dt} = L_2 \frac{dI_2}{dt} \quad , \tag{A.14}$$

$$L_2 \simeq \mu_o \frac{N}{\ell} \pi R_o^2 \quad . \tag{A.15}$$

We recall, that this value of the inductance in the homogeneous field approximation is chosen equal to the actual one.

For the evaluation of the flux changes produced by the eddy currents we have to return to Fig. A of this Appendix. The induced voltage in the m-th winding of the M-th pancake due to change of eddy currents in all windings with $s \geqslant m$ is:

$$\mu_o \frac{N}{\ell} \left[\sum_{s=m}^{n} 2\pi(a - 2sd)2 \int_0^d \frac{\ell \dot{J}_{Fs}}{N} x dx - 2\pi(a - 2md) \int_0^d \frac{\ell}{N} \dot{J}_{Fm} x dx \right] .$$

Like in the preceding section we replace J_{Fm} by $J_{F1} = J_{Fm}/(m - \frac{1}{2})$ (cf. Eq. (A.6)):

$$\mu_o \frac{N}{\ell} 4\pi d \left[\int_0^d \frac{\ell}{Nd} \dot{J}_{F1} x dx \right] \left[\sum_{s=m}^{n} (s - \tfrac{1}{2})(a - 2sd) - \tfrac{1}{2}(m - \tfrac{1}{2})(a - 2md) \right] .$$

The total induced emf in the primary due to these eddy currents is:

$$\frac{d\phi_{11F}}{dt} = \mu_o \frac{N^2 n^2 \pi a^2}{\ell} \sum_{m=1}^{n} \frac{(m - \tfrac{1}{2})^2 4d(a - 2md)}{n^2 a^2} \left[\int_0^d \frac{\ell \dot{J}_{F1}(x)}{dN} x dx \right] \equiv$$

$$\equiv F_1 \left[\int_0^d \frac{\ell \dot{J}_{F1}}{dN} x dx \right] \quad , \tag{A.16}$$

where F_1 is the coefficient of "Foucault"-inductance:

$$F_1 = \mu_o \frac{N^2 n^2 \pi a^2}{\ell} \sum_{m=1}^{n} \frac{(m - \tfrac{1}{2})^2 4d(a - 2md)}{n^2 a^2} \simeq 3.30 \text{ mH} \quad . \tag{A.17}$$

Analogously we find:

$$\frac{d\phi_{12F}}{dt} = F_{12} \left[\int_0^d \frac{\ell}{d} \dot{J}_{F2} x dx \right] \text{ and } \frac{d\phi_{21F}}{dt} = F_{12} \left[\int_0^d \frac{\ell}{Nd} \dot{J}_{F1} x dx \right] \quad , \tag{A.18}$$

$$\frac{d\phi_{22F}}{dt} = F_2 \left[\int_0^d \frac{\ell}{d} \dot{J}_{F2} x dx \right] \quad , \tag{A.19}$$

where the coefficients F_{12} and F_2 have the magnitudes:

$$F_{12} = \mu_o \frac{Nn\pi a^2}{\ell} \sum_{m=1}^{n} \frac{(m - \frac{1}{2}) 4d(a - 2md)}{na^2} \simeq 19.1 \ \mu H \quad , \tag{A.20}$$

$$F_2 = \mu_o \frac{\pi(a^2 - (a - 2nd)^2)}{\ell} \simeq 0.167 \ \mu H \quad . \tag{A.21}$$

Finally, the contribution to the emf in the secondary winding due to the eddy currents in the Bitter magnet will be calculated under the assumption that the Bitter plates have a uniform thickness d_B and extend from $R = R_-$ to R_+. We take d_B equal to the thickness of the actual wedge-shaped Bitter plates at a radius of $0.7 (R_+ - R_-)$. Though the Bitter magnet contains practically no air volume, there is some stray inductance due to the presence of the insulation plates. We shall take this into account through a correction factor g ($\simeq 0.9$). We find:

$$\frac{d\phi_B}{dt} = F_B \left[\int_0^{d_B} \frac{\ell}{d_B} \dot{J}_{FB} x dx \right] \text{ with } F_B = \mu_o g \frac{\pi(R_+^2 - R_-^2)}{\ell} \simeq 0.61 \ \mu H \ . \tag{A.22}$$

Substitution of the expressions for the various flux changes into the Eqs. (3a) and (3b) leads to:

$$L_1 \dot{I}_1 + F_1 \left[\int_0^d \frac{\ell}{Nd} \dot{J}_{F1} x dx \right] + M_{12} \dot{I}_2 + F_{12} \left[\int_0^d \frac{\ell}{d} \dot{J}_{F2} x dx \right] + R_1 i_1 = e, \tag{A.23}$$

$$L_2 \dot{I}_2 + F_2 \left[\int_0^d \frac{\ell}{d} \dot{J}_{F2} x dx \right] + F_B \left[\int_0^{d_B} \frac{\ell}{d_B} \dot{J}_{FB} x dx \right] +$$

$$+ M_{12} \dot{I}_1 + F_{12} \left[\int_0^d \frac{\ell}{Nd} \dot{J}_{F1} x dx \right] + R_2 i_2 = 0 \quad . \tag{A.24}$$

These transformer equations, together with the Eqs. (A.4), (A.7), and (A.8), form a complete set. The numerical values for the various inductances of the Alcator aircore transformer are listed in Table A.

TABLE A

	calculated	measured		calculated	measured
L_1	5.70 mH	6 mH	-	-	-
M_{12}	27.2 µH	27 µH	F_1/L_1	0.577	0.55
L_2	1.37 µH	-	F_{12}/M_{12}	0.70	0.69
F_1	3.3 mH	3.3 mH	F_2/L_2	0.122	-
F_{12}	19.1 µH	19 µH	F_B/L_2	0.446	-
F_2	0.167 µH	-	$(F_q + F_B)/L_2$	0.565	-
F_B	0.61 µH	-	-	-	-

Note that the ratios F/L indicate the relative influence of the copper.

In Appendix B, several characteristic quantities of aircore transformers of the Alcator pancake type are calculated as a function of the relative copper volume.

A P P E N D I X B

OPTIMALIZATION OF THE PANCAKE-TYPE AIRCORE TRANSFORMER

In Appendix A various coefficients of inductance are formally expressed in terms of N, ℓ, a, n, and d. Also other characteristic quantities as stress, heat/volume, time constants etc. can be expressed in terms of the parameters. With the help of these expressions we can evaluate the variation of these quantities with one or more of the parameters. We will express these quantities specifically in terms of N/ℓ, N, a, n, $\beta = 2nd/a$; the last parameter β is a measure of the relative "copper part" of the primary of the aircore transformer.

Firstly, we list several quantities:

$$\text{Flux } \Phi_o = M_{12} I_o = \mu_o \frac{Nn\pi a^2 I_o}{\ell} g_M(\beta,n) \quad ;$$

$$g_M = \left[1 - \beta\left(1+\frac{1}{n}\right)\left(1-\frac{\beta}{3}\left(1+\frac{1}{2n}\right)\right)\right] = 1/g_{i_o} \quad ;$$

Mutual inductance

$$M_{12} = \mu_o \frac{Nn\pi a^2}{\ell} g_M \quad ;$$

primary inductance

$$L_1 = \mu_o \frac{N^2 n^2 \pi a^2}{\ell} g_L(\beta,n) \quad ;$$

$$g_L = \left[\left(3+\frac{1}{n}-\frac{1}{n^2}\right)\left(1+\frac{1}{n}\right)\beta^2 - \frac{4}{3}\left(1+\frac{1}{n}\right)\left(1-\frac{1}{4n}\right)\beta + 1\right] \quad ;$$

coupling factor

$$k^2 = \frac{M_{12}^2}{L_1 L_2} = \frac{\mu_o \pi a^2}{\ell L_2} g_k \quad , \quad g_k = g_M^2/g_L \quad ;$$

peak voltage over the breaker

$$\hat{V}_b = \frac{L_1 I_o}{\tau_1} = \mu_o \frac{N^2 n^2 \pi a^2}{\ell} I_o g_L(\beta,n) = \frac{Nn}{\tau_1} \Phi_o g_{\hat{V}} \; ; \quad g_{\hat{V}} = g_L/g_M \; ;$$

stress in case of total cooperation of all windings

$$\sigma_{coop} = \frac{\Phi_o^2}{\mu_o \pi^2 a^4} g_{\sigma_c} \quad ; \quad g_{\sigma_c} = \frac{1 - \beta(1 + \frac{1}{n})(\frac{2}{3} - \frac{1}{6n})}{4\beta g_M^2} \quad .$$

In Fig. B these quantities g have been plotted as functions of β for $n = 6^1/_3$. We observe that the value of $\beta \approx 0.55$ chosen for Alcator is the optimal value as far as stress is concerned. However, if we reduce β to 0.35, the stress is only 15% higher. In other words, a reduction of the flux Φ with 7% yields the same stress value. At the same time, however, the total power needed and the breaker rating are reduced by 20% and also the total mechanical preloading can be appreciably less.

In conclusion we may say that the most optimal design is that of the Alcator (apart from the fact that the windings should be laminated because of the eddy currents). An appreciably smaller β, however, is not much inferior and may be appreciably cheaper in design for coil, generator, and breaker. Besides, the higher coupling factor could be advantageous in the beginning of the discharge.

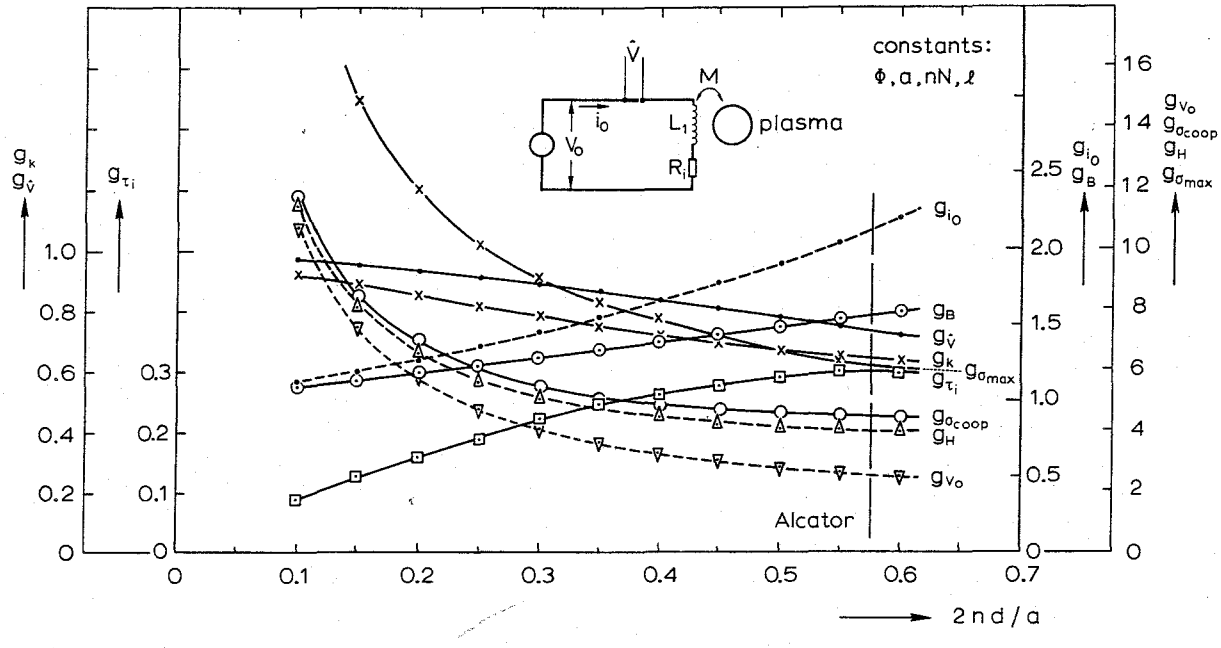

Fig. B Typical quantities for a pancake-aircore transformer as a function of the relative copper volume, $\beta = 2\,nd/a$.

breaker "quality"

$$\hat{V}_b I_o = \frac{\ell \phi_o^2}{\mu_o \pi a^2 \tau_1} g_B \quad ; \quad g_B = g_L / g_M^2 \quad ;$$

stored inductive power

$$\frac{1}{2} L_1 I_o^2 = \frac{\ell \phi_o^2}{2\mu_o \pi a^2} g_B \quad ;$$

internal resistance

$$R_i = \eta \frac{N^2 n^2}{\ell} 2\pi \, g_{R_i} \quad ; \quad g_{R_i} = \frac{2 - (1 + \frac{1}{n})\beta}{2\beta} \quad ;$$

internal time constant

$$\tau_i = \frac{L_i}{R_i} = \frac{\mu_o}{\eta} \frac{a^2}{2} g_{\tau_i} \quad ; \quad g_{\tau_i} = g_L / g_R \quad ;$$

heat/unit volume

$$H = \frac{\frac{1}{2} R_i I_o^2 \tau_i}{\pi a^2 \ell \beta \left(2 - (1 + \frac{1}{n})\beta\right)} = \frac{\eta N^2 n^2 I_o^2 \tau_i}{a^2 \ell^2 \beta^2} = \frac{\Phi_o^2}{2\mu_o \pi^2 a^4} g_H \; ; \; g_H = \frac{g_{\tau_i}}{g_M^2 \beta^2} \; ;$$

D.C. generator voltage

$$V_o = I_o R_i = \frac{\eta N^2 n^2}{\ell} I_o \cdot 2\pi g_{R_i} = \frac{\eta 2Nn}{a^2} \Phi_o g_{V_o} \quad ; \quad g_{V_o} = g_{R_i} / g_M \quad ;$$

maximum stress (no cooperation): $\boxed{\beta \geq \frac{1}{2}/(1 - 1/4n)}$

$$\sigma_{max} = \mu_o \frac{N^2 n^2 I_o^2}{\ell^2} \frac{(1 - \beta/2n)}{4\beta^2} = \frac{\Phi_o}{\mu_o 2\pi^2 a^4} g_{\sigma_{max}} \quad ;$$

$$g_{\sigma_{max}} = \frac{(1 - \beta/2n)^2}{2\beta^2} / g_M^2 \quad ;$$

$$\boxed{\beta \leq \tfrac{1}{2}/(1 - 1/4n)}$$

$$\sigma_{max} = \mu_o \frac{N^2 n^2 I_o^2}{\ell^2} \left[\frac{(1 - \beta)(2 - 1/n)}{2\beta}\right] = \frac{\Phi_o^2}{\mu_o \pi^2 a^4 2} g_{\sigma_{max}} \quad ;$$

$$g_{\sigma_{max}} = \frac{(1 - \beta)(2 - 1/n)}{\beta} / g_M^2 \quad ;$$

A P P E N D I X C

A NON-CONSTANT PLASMA RESISTANCE IN THE FORMATION PHASE OF THE DISCHARGE

In Section 6 the time dependence of the plasma resistance is neglected in order to obtain a clear insight in the net effect of the eddy currents in the aircore transformer and in the Bitter magnet. However, in the initial stage of the discharge the plasma resistance is a strong function of time; it is large in the very beginning of the discharge and after completion of the ionization phase it decreases fast with increasing temperature. It is clear that this will affect the time dependence of the plasma current; in the presence of eddy currents this effect may be even more pronounced as the eddy currents affect the initial rise of the plasma current (see Section 6). It is possible that the resulting change in the time dependence of the power input increases the duration of the ionization phase, which means an enhanced loss of flux. To get some insight in these problems, essential for optimum design of the aircore transformer, we shall present here a rather qualitative model. Basically we shall make two simplifications: we neglect particle losses and we assume that at any time enough energy is available to supply ionization and excitation losses. These assumptions decouple the multiplication process from particle and energy balances.

The initial stage of the discharge can be separated into two distinct phases: in phase A, where ionization causes the very low (but finite) initial electron-number density to rise to a level where electron-ion collisions start to dominate over electron-neutral collisions and in phase B, where the ionization is completed. Two additional assumptions enable us to evaluate the current in and the duration of these two phases: we assume that during phase A, E/p is constant and that during phase B the electron temperature is constant at a value of about 10 eV. After phase B the ionization is complete and the ohmic heating leads to a fast increase in electron temperature.

The model must be interpreted as an optimistic characterization of the start of the discharge as particle loss and influx of neutrals are neglected. These assumptions are not unreasonable for phase A, when n_e increases fast; however, during phase B the assumptions of negligible losses and sufficient power input may well be in-

validated[3]. Therefore, the analysis will lead to minimum requirements on the flux. At the same time we shall get some indication about the additional effect of the eddy currents.

The resistive loss of flux during the initial phase

$$\Delta\phi_A + \Delta\phi_B \equiv - \int_0^{t_A} I_2 R_{2_A} dt - \int_{t_A}^{t_B} I_2 R_{2_B} dt \qquad (C.1)$$

leads to a reduction of the attainable plasma current I_2 in the final hot phase, according to ($t \gg \tau_1$; $I_1(o) \simeq 0$) (cf. Eq. (16)):

$$L_2 I_2 \Big|_t = M_{12}^{(o)} I_1(o) - \int_0^t I_2 R_2 dt \quad , \qquad (C.2)$$

where $M_{12}^{(o)}$ is the low-frequency mutual inductance.

An estimate of the extra contribution to this loss of flux, due to the high value of the time-dependent resistance can be estimated by the calculation of:

$$\Delta\phi_A = - \int_0^{t_A} I_2(t) \left[R_{2_A}(t) - R_2(\infty)\right] dt \simeq - \int_0^{t_A} I_2(t) R_{2_A}(t) dt, \qquad (C.3a)$$

where $R_2(\infty)$ is the small resistance of the plasma during the hot phase and

$$\Delta\phi_B \simeq - \int_{t_A}^{t_B} I_2(t) R_{2_B} dt \quad . \qquad (C.3b)$$

The normalized loss of flux

$$\frac{\Delta\phi}{\phi_o} = \frac{\int_0^t I_2 R_2 dt}{M_{12}^{(o)} I_o} \quad ,$$

is an indication of the extra reduction in the attainable plasma current and will be estimated for phases A and B, both without and with eddy currents.

Another quantity that needs consideration is the power input $I_2^2 R_2$ which should be sufficient to supply the required excitation and ionization losses during the build-up stage; for both phases this quantity will be compared with the ionization losses.

For these two calculations an estimate of the resistivity of the plasma is essential. This is the starting point of the present discussion.

In phase A, the electron-neutral collision-dominated regime, the neutral number density is high. Electrons lose momentum in e-o collisions and we can obtain multiplication factors from classical data[4]. The multiplication factor β (number of ionizations per second) is shown in Fig. C.1 as a function of $\hat{E}/p$ for molecular hydrogen H_2 and helium. In the initial stage of a Tokamak discharge the electric field strength E is typically between 5 V/m and 15 V/m and the filling pressure for hydrogen is 2 to 5×10^{-4} Torr. The quoted E-values relate to open loop voltages: for the interior of the plasma column smaller values can be expected. Corresponding $\hat{E}/p$-values are in the range of 10^4 to 7×10^4 V/m Torr and a typical β/p-value is:

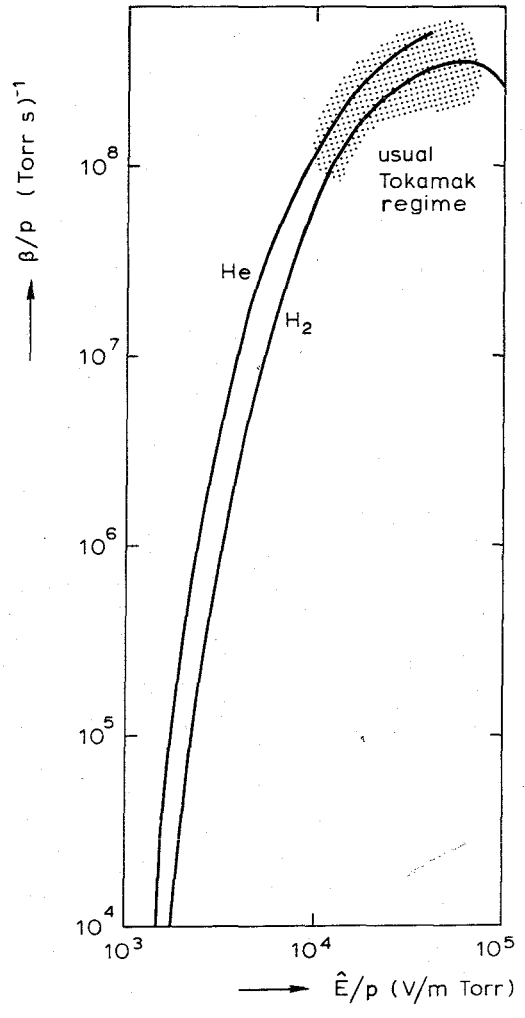

Fig. C.1 β/p as a function of reduced electric field strength $\hat{E}/p$ for H_2 and He.

$$\beta/p \simeq 2 \times 10^8 \text{ (Torr s)}^{-1} . \qquad \text{(C.4)}$$

Throughout phase A, this value of β/p is assumed to be constant. This is quite reasonable because $p \simeq p_o \simeq$ constant as well as $\hat{E} \simeq$ constant if the primary time constant τ_1 is long compared to the duration of phase A, t_A, which in general is the case. We assume that the initial electron-number density is non-zero; it may, however, be very small.

In the absence of loss (or more precisely, a characteristic diffusion time should be longer than $1/\beta$), the electron-number density $n_e(t)$ and corresponding ionization degree $\alpha(t)$ increase according to:

$$n_e(t) = n_e(o)e^{\beta t} \quad ; \quad \alpha(t) \equiv \frac{n_e(t)}{2n_{H_2}(o)} = \alpha(o)e^{\beta t} \quad . \qquad (C.5)$$

Phase A is supposed to be terminated when electron-ion collisions start to dominate over electron-neutral collisions, i.e,

$$\nu_{e-o}(t) = 0.43 \times 10^{10}\, p_o(\text{Torr } H_2) \simeq 0.12 \times 10^{-12}\, n_{H_2}(t) \quad , \qquad (C.6)$$

$$\nu_{e-i}(t) \simeq 2 \times 10^{-11} \frac{n_e}{T_e^{3/2}\,(\text{eV})} \quad , \qquad (C.7)$$

$$n_e(t_A) \equiv n_{eA} = 2 \times 10^{20} \times p_o \times T_e^{3/2}\,(\text{eV}) \text{ and } \alpha_A \simeq \frac{T_{eA}^{3/2}}{350} \quad , \qquad (C.8)$$

where ν is the collision frequency.

The duration of phase A, t_A, is short, even for a small initial ionization degree:

$$\beta t_A = \ln \frac{\alpha(t_A)}{\alpha(o)} = \ln [\alpha_A] - \ln [\alpha(o)] \quad , \qquad (C.9)$$

and is typically a few tens of a millisecond ($\beta t_A \sim 10$ à 15). In phase A the plasma resistivity is dominated by the electron-neutral momentum transfer:

$$\eta_{e-o}(t) = \frac{3 \times 10^7\, \nu_{e-o}(t)}{n_e(t)} = \frac{1.6 \times 10^{-6}}{\alpha(o)}\, e^{-\beta t} \quad , \qquad (C.10)$$

so that the resistance of the plasma is given by ($T_{eA} \simeq 10$ eV):

$$R_{2_A}(t) = \eta(t)\, \frac{2\pi R_o}{\pi r_p^2} \simeq \frac{2R_o\, 1.6 \times 10^{-6}}{r_p^2\, \alpha(o)}\, e^{-\beta t} = \frac{2R_o\, 1.1 \times 10^{17} p_o(\text{Torr}, H_2)}{r_p^2\, n_e(t)} \quad , \qquad (C.11)$$

and the secondary time constant is (for aspect ratio $A = \frac{R_o}{r_p} \simeq 5$):

$$\tau_2(t) = \tau_2(o)e^{\beta t} = \frac{\mu_o R_o \ln[1.38\, R_o/r_p]}{\frac{2R_o}{r_p^2} \cdot \frac{1.6 \times 10^{-6}}{\alpha(o)}\, e^{-\beta t}} = 0.85\, r_p^2 \cdot \alpha(o)e^{\beta t} \quad . \qquad (C.12)$$

The transformer equation for a weakly coupled transformer ($k^2 \ll 1$) in the absence of eddy currents and for constant plasma inductance (no appreciable pinching during t_A) is (cf. Eq. (16) and Eq. (20)):

$$L_2 \frac{dI_2}{dt} + R_2(t) I_2 = \frac{M_{12} I_o}{\tau_1} e^{-t/\tau_1} \simeq \frac{M_{12} I_o}{\tau_1} \quad . \tag{C.13}$$

The solution with initial conditions (15) is:

$$I_2(t) = \frac{M_{12} I_o}{L_2 \beta \tau_1} \cdot \exp\left[\frac{e^{-\beta\tau}}{\beta\tau_{20}}\right] \int_0^{\beta t} \exp - \left[\frac{e^{-\beta t'}}{\beta\tau_{20}} + \frac{t'}{\tau_1}\right] d\beta t' \quad ,$$

or in terms of exponential integrals[5]:

$$E_1(x) \equiv \int_x^{\infty} \exp\,(e^{-x'})\, dx' \quad ,$$

we find for $\frac{t'}{\tau_1} \ll 1$

$$I_2(t) = \frac{M_{12} I_o}{L_2 \beta \tau_1} \cdot \exp\left[\frac{e^{-\beta t}}{\beta\tau_{20}}\right] \cdot \left[E_1\left(\frac{e^{-\beta t}}{\beta\tau_{20}}\right) - E_1\left(\frac{1}{\beta\tau_{20}}\right)\right] \quad . \tag{C.14}$$

From Eq. (C.12) we recall that for $T_e \sim 10$ eV (cf. Eq. (C.8)):

$$\frac{e^{-\beta t_A}}{\beta\tau_{20}} = \frac{1}{\beta\tau_2(t_A)} \equiv \frac{1}{\beta\tau_{2A}} = \frac{1}{\beta \cdot 0.85\, r_p^2 \alpha_A} = \frac{1}{2.7 \times 10^3\, r_p^2} \ll 1 \quad . \tag{C.15}$$

Note, that $\beta\tau_{2A}$ depends only on T_{eA}, p_o, and r_p^2 and weakly on $\hat{E}/p$. Since $T_{eA} \sim 10$ eV and $p_o \sim 2 \times 10^{-4}$ Torr the only dependence is on plasma radius, and such, that the larger r_p^2 the better inequality (C.15) is fulfilled; for Alcator $\beta\tau_{2A} \approx 30$. Under condition (C.15) the plasma current at $t = t_A$ is*:

$$I_2(t_A) \simeq \frac{M_{12} I_o}{L_2 \beta \tau_1} \left[E_1\left(\frac{1}{\beta\tau_{2A}}\right) - E_1\left(\frac{1}{\beta\tau_{20}}\right)\right] \quad . \tag{C.16}$$

---

*) Note that in the presence of Foucault currents $\beta\tau_{2A}$ is reduced to:

$$\beta\tau_{2A}^{(F)} = 2.7 \cdot 10^3\, r_p^2 \left(1 - \frac{F_2}{L_2} - \frac{F_B}{L_2}\right) \quad .$$

For the usual case of weak preionization $\beta\tau_{20} \simeq 3.4 \times 10^2\, \alpha(o) \ll 1$, so that the plasma current at $t = t_A$, $I_2(t_A)$ can be approximated by ($E_1(1/\beta\tau_{20})$ can be neglected):

$$I_2(t_A) \simeq \frac{M_{12}I_o}{L_2\beta\tau_1}\left[\frac{1}{\beta\tau_{2A}} + \beta t_A - \ln\left(\frac{1}{\beta\tau_{20}}\right) - 0.577\right] \simeq \frac{M_{12}I_o}{L_2\beta\tau_1}\,\beta t_A \quad . \qquad (C.17)$$

For a good preionization, but $\alpha(o)$ still smaller than α_A, $\beta\tau_{20} \gtrsim 1$, which is identical to $\alpha(o) > 3 \times 10^{-5}/r_p^2$ according to Eq. (C.12), we find for the plasma current (C.16):

$$I_2(t_A) \simeq \frac{M_{12}I_o}{L_2\beta\tau_1}\left[\beta t_A - \frac{1 - e^{-\beta t_A}}{\beta\tau_{20}}\right] = \frac{M_{12}I_o}{L_2\beta\tau_1}\left[\beta t_A - \left(\frac{1}{\beta\tau_{20}} - \frac{1}{\beta\tau_{2A}}\right)\right] \quad . \qquad (C.18)$$

The loss of flux ($\Delta\phi_A$) can be obtained by noting that:

$$\Delta\phi_A = -\int_0^{t_A} I_2 R_2(t)\,dt \simeq -\int_0^{t_A}\left\{-L_2\frac{dI_2}{dt} + \frac{M_{12}I_o}{\tau_1}e^{-t/\tau_1}\right\}dt \simeq -\frac{M_{12}I_o}{\tau_1}t_A + L_2 I_2(t_A)$$

and is equal to ($1/\beta$, $\tau_{20} \ll t_A \ll \tau_1$)

$$\left.\begin{aligned} \frac{\Delta\phi_A}{\phi_o} &\simeq -\frac{\ln\left[\frac{1}{\beta\tau_{20}}\right] + 0.577}{\beta\tau_1} \simeq -\frac{\ln\left[\frac{1}{\beta\tau_{20}}\right]}{\beta\tau_1} \ll 1 \quad ; \ \beta\tau_{20} \ll 1 \\ &\qquad\qquad\qquad\qquad\qquad\qquad\qquad\qquad\qquad\qquad \text{weak preionization} \\ \frac{\Delta\phi_A}{\phi_o} &\simeq -\frac{\left[\frac{1}{\beta\tau_{20}} - \frac{1}{\beta\tau_{2A}}\right]}{\beta\tau_1} \simeq -\frac{1}{\beta\tau_1\beta\tau_{20}} \lll 1 \quad ; \ \beta\tau_{20} \gtrsim 1 \\ &\qquad\qquad\qquad\qquad\qquad\qquad\qquad\qquad\qquad\qquad \text{good preionization} \end{aligned}\right\} \qquad (C.19)$$

where $\phi_o = M_{12}I_o$ is the available flux.

In this model the loss of flux will be small (especially in the second case) as $\beta\tau_1 \gg 1$ (in the order of 10^2 to 10^3); even in the case of weak preionization it is a few % at maximum. For small primary time constants (cf. $\tau_1 \sim 2$ msec for ST-Tokamak*) this loss may be an important factor, and a good preionization may be essential. Note that the loss of flux originates from the small deviation of the plasma current with respect to a linear increase with time (see right-hand side of Eq. (C.17)). This linear dependence would be the solution for a constant very low plasma resistance.

*) Note, however, that an assumption of low coupling factor has been made.

In the presence of eddy currents we find for $\tau_s \ll \tau_1$ and $\tau_B \ll \tau_1$:

$$\frac{\Delta\phi}{\phi_o} \simeq - \frac{\ln\left[\frac{1}{\beta\tau_{20}(1 - F_2/L_2 - F_B/L_2)}\right]}{\beta\tau_1} \cdot \frac{(1 - F_{12}/M_{12})}{(1 - F_1/L_1)} \quad ; \quad \beta\tau_{20}\left(1 - \frac{F_2}{L_2} - \frac{F_B}{L_2}\right) \ll 1 \ , \tag{C.19^F}$$

$$\frac{\Delta\phi}{\phi_o} \simeq - \frac{1}{\beta\tau_1 \cdot \beta\tau_{20}} \cdot \frac{(1 - F_{12}/M_{12})}{(1 - F_1/L_1)(1 - F_2/L_2 - F_B/L_2)} \quad ; \quad \beta\tau_{20}\left(1 - \frac{F_2}{L_2} - \frac{F_B}{L_2}\right) \gtrsim 1 \ .$$

In both cases the eddy currents in the primary and in the Bitter magnet increase the loss of flux in phase A of the initial stage.

The dissipation $I_2^2 R_2$ in the plasma should be sufficient to supply the required ionization and excitation losses:

$$I_2^2 R_2 > n_e(t)\ \varepsilon_{ion}(\text{volume})\ \beta = n_e(t)\ \varepsilon_{ion} 2\pi^2 R_o r_p^2 \beta \quad . \tag{C.20}$$

With Eq. (C.10) we can rewrite $n_e(t) r_p^2 = 2.2 \times 10^{17} p_o R_o / R_2(o) e^{-\beta t}$, and with $\varepsilon_{ion} \sim 10^{-17}$ joule and $\beta/p \sim 2\times10^8$ we find:

$$\frac{M_{12} I_o}{\beta^2 \tau_1 \tau_{20}} \beta t e^{-\beta t} > 5 \times 10^{-4} R_o \quad . \tag{C.21}$$

The function $e^{-\beta t}\ \beta t$ is minimal for maximum βt (the function is also a minimum for $\beta t = 0$, but averaged over the first e-folding time it is not small), so

$$\frac{M_{12} I_o}{\beta\tau_{20}\beta\tau_1} e^{-\beta t_A} \beta t_A > 5 \times 10^{-4} R_o \quad . \tag{C.22}$$

Since $\beta\tau_{20} e^{\beta t_A} = \beta\tau_{2A} = 2.7 \times 10^3 r_p^2$ (C.15) in the absence of eddy currents, we find:

$$M_{12} I_o \frac{t_A}{\tau_1} \geqslant 1.4 \times r_p^2 R_o \simeq 0.7 \times 10^{-2} \quad \text{(Alcator)} \quad . \tag{C.23}$$

This requirement is mostly fulfilled within a reasonable margin; e.g. for Alcator: $M_{12} I_o = \Phi_o = 1$ Vsec, $t_A = 0.2$ msec, $\tau_1 \simeq 15$ msec. Inclusion of losses may however render this marginally. Note, that an upper limit is imposed on the primary time constant: it should not be too long.

In the presence of eddy currents the requirement (C.22) is relaxed:

$$\frac{M_{12}I_o e^{-\beta t_A}\beta t_A}{\beta\tau_{20}\beta\tau_1} \times \left[\frac{1 - F_{12}/M_{12}}{\left(1 - \frac{F_2}{L_2} - \frac{F_B}{L_2}\right)\left(1 - \frac{F_1}{L_1}\right)}\right] > 5 \times 10^{-4} R_o \quad , \qquad (C.22^F)$$

or

$$M_{12}I_o \frac{t_A}{\tau_1}\left[\frac{1 - F_{12}/M_{12}}{\left(1 - \frac{F_2}{L_2} - \frac{F_B}{L_2}\right)\left(1 - \frac{F_1}{L_1}\right)}\right] = 1.7\, M_{12}I_o \frac{t_A}{\tau_1} > 0.7 \times 10^{-2}. \qquad (C.23^F)$$

Observe that especially eddy currents in the Bitter magnet are advantageous. This is quite understandable, as the reduction of the secondary inductance yields an increase in the rate of rise of the plasma current and therewith the power input.

In phase B where electron-ion collisions dominate, the electron temperature is assumed to be roughly constant at a value of 10 eV. It is difficult to estimate the duration of this period: $t_B - t_A = \Delta t_B$. Besides dissociation and ionization of molecular hydrogen, ionization of atomic hydrogen will play a role[4]:

$$\left.\begin{array}{ll} \text{(a)} & H_2 + e \rightarrow H + H + e \\ \text{(b)} & H_2 + e \rightarrow H_2^+ + e + e \\ \text{(c)} & H_2^+ + e \rightarrow (H_2^+)^* + e \rightarrow H + H^+ + e \text{ (dominant process)} \\ & \qquad\qquad \rightarrow H^+ + H^+ + 2e \\ \text{(d)} & H + e \rightarrow H^+ + e + e \quad . \end{array}\right\} \qquad (C.24)$$

We observe (Fig. C.2) that $\sigma_b \sim 1.5\, \sigma_d$ and that the dissociation processes (a) and (c) are relatively fast for the electron energies under consideration ($T_e \sim 10$ eV). Therefore, we estimate the time dependence of n_e, as if already at $t = t_A$ all the molecular hydrogen was dissociated and the only important process is (d):
$n_H(t_A) \simeq 2n_{H_2}(o)$

$$\frac{dn_e}{dt} = n_e(t) n_H(t) \langle\sigma v_e\rangle_{\text{ion H}} \simeq n_e(t) \left[2n_{H_2}(o) - n_e(t)\right]\langle\sigma v_e\rangle_{\text{ion H}} \quad ,$$

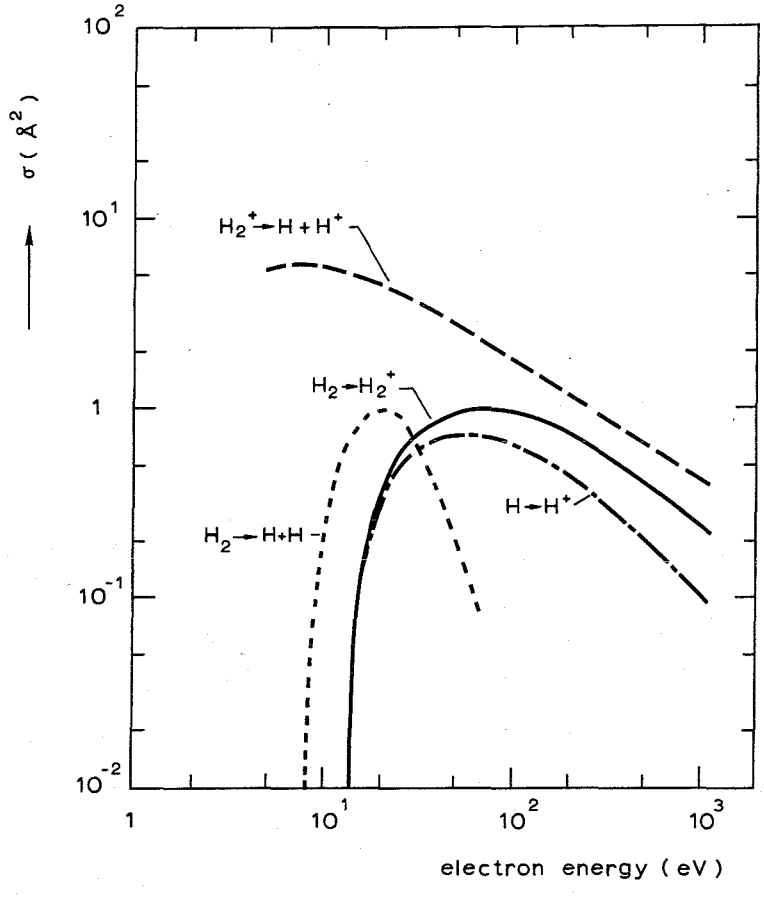

Fig. C.2 Cross sections for dissociation and ionization of atomic and molecular hydrogen.

or

$$\frac{d\alpha(t)}{dt} = \alpha(t)\left[1-\alpha(t)\right]2n_{H_2}(o)\langle\sigma v_e\rangle_{\text{ion H}} = \alpha(t)\left[1-\alpha(t)\right]\beta_H \quad , \tag{C.25}$$

where

$$\beta_H = 2n_{H_2}(o)\langle\sigma v_e\rangle_{\text{ion H}} \simeq 1.5\times 10^8 \times p_o \ (\text{Torr}, H_2) \quad . \tag{C.26}$$

In this model the electron-number density rises according to:

$$\alpha(t) \equiv \frac{n_e(t)}{2n_{H_2}(o)} \simeq \frac{1}{1+\frac{1}{\alpha_A}\exp\left[-\beta(t-t_A)\right]} \quad . \tag{C.27}$$

The duration of phase B can be estimated to be twice the time required to ionize 95% of H according to (C.26):

$$t_B - t_A \simeq 2\left[\ln \frac{1}{1-\alpha(t_B)} + \ln \frac{1}{\alpha_{A-}}\right] \sim \frac{10}{\beta_H} \quad . \tag{C.28}$$

Like phase A, phase B takes approximately a few 100 μsec, provided that the power input is sufficient to supply the ionization and excitation losses. Note that in phase B the electric field strength $\hat{E}$ should be below the Dreicer limit.

During phase B, T_e is assumed to be constant and equal to ~ 10 eV. Therefore, also the plasma resistivity is constant and equal to (Eq. (C.7)):

$$\eta_B(t) \simeq 6 \cdot 10^{-4}\ T_e^{-3/2}\ \Omega m \quad . \tag{C.29}$$

The plasma resistance is equal to:

$$R_{2B} \simeq \eta_B(t) \cdot \frac{2R_o}{r_p^2} \simeq 100\,\eta \quad \text{(Alcator)} \tag{C.30}$$

and the secondary time constant is for aspect ratio $A = \frac{R_o}{r_p} \sim 5$

$$\tau_{2B} = \frac{L_2}{R_{2B}} = \frac{\mu_o r_p^2 \ln[1.38\ R_o/r_p]}{1.2 \cdot 10^{-3} T_e^{-3/2}} = 0.7\ r_p^2 \quad . \tag{C.31}$$

Observe that this time constant may be smaller than the primary time constant τ_1; e.g. for Alcator $\tau_{2B} \simeq 7$ msec, $\tau_1 \sim 15$ msec. In the absence of eddy currents the plasma current can be calculated from Eqs. (16) with initial conditions:

$$I_{1A} = I_o e^{-t_A/\tau_1} \simeq I_o \left(1 - \frac{t_A}{\tau_1}\right) \text{ and } I_{2A} = \frac{M_{12} I_o}{L_2} \frac{t_A}{\tau_1}\ , \text{ with } \frac{t_A}{\tau_1} \ll 1 \quad . \tag{C.32}$$

The Laplace transform of the plasma current is (compare Eq. (18)):

$$\left.\begin{aligned} I_{2p} &= \frac{M_{12}\tau_2}{D} I_{1A} + \frac{(1+p\tau_1)\tau_2 - p\,\frac{M_{12}^2}{R_1 R_2}}{D} I_{2A} \\ \text{with} \\ D &= (1+p\tau_1)(1+p\tau_2) - p^2 \frac{M_{12}^2}{R_1 R_2} \equiv (1+p\tau_I)(1+p\tau_{II}) \quad . \end{aligned}\right\} \tag{C.33}$$

So, with $t' \equiv t - t_A$.

$$I_2(t') = \frac{M_{12}I_{1A}}{L_2}\,\frac{e^{-t'/\tau_{II}} - e^{-t'/\tau_I}}{(\tau_{II}-\tau_I)/\tau_2} + I_{2A}\left[\frac{(\tau_I-\tau_1)e^{-t'/\tau_I} - (\tau_{II}-\tau_I)e^{-t'/\tau_{II}}}{\tau_I - \tau_{II}}\right].$$

Since for a weakly coupled transformer $\tau_1 \simeq \tau_I$, this reduces to

$$I_2(t') \simeq \frac{M_{12}I_{1A}}{R_2}\,\frac{e^{-t'/\tau_{II}} - e^{-t'/\tau_I}}{\tau_{II}-\tau_I} + \frac{M_{12}I_o}{L_2}\cdot\frac{t_A}{\tau_1}\,e^{-t'/\tau_{II}} \quad , \text{(C.34)}$$

and the loss of flux is

$$\Delta\phi_B = \int_0^{t_B-t_A} R_2 I_2(t')\,dt' \simeq M_{12}I_{1A}\,\frac{t_B^2 - t_A t_B}{\tau_I \tau_{II}} \simeq M_{12}I_o\,\frac{t_B^2 - t_A t_B}{\tau_1 \cdot \tau_{2B}} \quad . \qquad \text{(C.35)}$$

The loss of flux and therefore the reduction of attainable plasma current is small; it amounts to a few % at maximum. In the presence of eddy currents the loss of flux is enhanced by a factor of f_k:

$$f_k = \frac{1 - F_{12}/M_{12}}{(1 - F_1/L_1)\,(1 - F_2/L_2 - F_B/L_2)} \simeq 1.7 \text{ (Alcator)}, \quad \text{so}$$

$$\Delta\phi_B^{(F)} = M_{12}I_o\,\frac{t_B^2 - t_B t_A}{\tau_1 \cdot \tau_{2B}}\,f_k \quad . \qquad (C.35^F)$$

However, as we will see later, the assumption of negligible losses and sufficient available power is quite optimistic in this phase. A lengthening of phase B will increase the loss of flux and thus lead to a reduction of the plasma current.

The requirement, that the ohmic heating power $I_2^2 R_2$ should be ample to supply the ionization and excitation losses is more difficult to meet in this phase. Obviously, the inequality is the same at the beginning of phase B as at the end of phase A at $t = t_A$. In phase B, the plasma current I_2 increases at most linearly with time (cf. Eq. (C.34)):

$$I_2(t) \simeq \frac{M_{12}I_o}{L_2}\,\frac{t}{\tau_1} \quad , \qquad \text{(C.36)}$$

and the plasma resistance is constant

$$R_{2B} = 6.10^{-4}\,T_e^{-3/2} \cdot 2R_o/r_p^2 \quad .$$

On the other hand, the ionization and excitation losses increase fast (cf. Eq. (C.25)):

$$\left(\frac{n_e}{t}\right)_{ion} \varepsilon_{ion} \cdot \text{volume} = 2n_{H_2}(o)\,\alpha(t)\,\big(1-\alpha(t)\big)\,\beta_H \varepsilon_{ion}\, 2\pi^2 r_p^2 R_o \quad ,$$

which reaches its maximum at $\alpha(t) = \frac{1}{2}$. The inequality $I_2^2 R_2 >$ Losses yields in this case

$$\frac{M_{12}^2 I_o^2 t^2}{L_2^2 \tau_1^2} \cdot R_2 > \frac{1}{2}\, n_{H_2}(o)\, \beta_H \varepsilon_{ion}\, 2\pi^2 r_p^2 R_o \quad . \tag{C.37}$$

With Eqs. (C.29), (C.31), aspect ratio $A \simeq 5$, $\varepsilon_{ion} \sim 10^{-17}$ joule $n_{H_2}(o) \sim 7\cdot 10^{18}/m^3$, $T_{eB} \sim 10$ eV, $\beta_H \simeq 1.5\times 10^8\, p_o$ (Torr) we find for the electric field strength

$$\hat{E} = \frac{M_{12} I_o}{\tau_1} > \frac{10 r_p^2 R_o}{t[\alpha(t)=\frac{1}{2}]} \simeq \frac{10 r_p^2 R_o}{t_A} \simeq \frac{1}{20 t_A} \simeq 250 \text{ V/m} \quad . \tag{C.38}$$

This has to be compared with the requirement that $\hat{E}$ has to be smaller than the Dreicer limit E_D in order to avoid runaway ($T_e \sim 10$ eV, $p_o \sim 2\cdot 10^{-4}$ Torr):

$$\hat{E} < E_{Dreicer} \simeq 2\cdot 10^{-17} n_e \simeq 250\, \alpha(t) \text{ V/m} \quad . \tag{C.39}$$

It is obvious that it is difficult to fulfill both requirements at the same time. Taking into account that the assumption of negligible losses is unrealistic we must conclude that this phase will take some more time. This will lead to an increase in the loss of Vsec. On the other hand, even if $\hat{E} < E_D$, the conditions will be favourable for the excitation of ion-acoustic turbulence, especially at the beginning of phase B. As a consequence, the resistance will be anomalously high, which will lead to an enhanced power input. In the presence of eddy currents the power input will increase by the factor of f_k^2 (cf. Eq. ($C.35^F$)), therewith suggesting a relaxing of the power requirement (C.38). However, also the induced voltage is increased, so in order to keep the field strength below the Dreicer limit, the primary time constant should be enlarged.

We will close the present discussion with the observation that a more elaborate and more detailed study of this phase should be undertaken to elucidate all these facets.